

Report AIFM

INTENSITY MODULATED RADIATION THERAPY (IMRT): DOSIMETRIC AND COMPUTATIONAL ASPECTS



*Gruppo di Lavoro
sulla Radioterapia
ad intensità modulata (IMRT)*

N.3 (2006)

Editor

Mauro Iori A.O.S. Maria Nuova, Reggio Emilia

Authors

Luigi Tana A.O. Universitaria Pisana, Pisa
Marta Paiusco A. O. S. Maria Nuova, Reggio Emilia
Fabrizio Banci Buonamici A. O. U. Careggi, Firenze
Stefania Cora A. O. Ospedale S. Bortolo, Vicenza
Cristina Garibaldi Istituto Europeo di Oncologia, Milano
Stéphane Chauvie A. S. O. Ordine Mauriziano, Cuneo
Laura Masi Casa di Cura S. Chiara, Firenze
Roberto Cirio INFN, Torino
Barbara Caccia Dipartimanto Tecnologie e Salute,
Istituto Superiore di Sanità, Roma
Simona Marzi Istituto Regina Elena, Roma
Ruggero Ruggieri A.O. Bianchi Melacrino Morelli, Reggio Calabria

Co-Authors

C. Andenna DIPIA-ISPEL, Roma
M. Mattia Dipartimento Tecnologie e Salute, ISS, Roma
C. Zicari DIPIA-ISPEL, Roma
M. Benassi Istituto Regina Elena, Roma
G. Sceni A.O. Bianchi Melacrino Morelli, Reggio Calabria
C. Raymondi Policlinico Monteluce, Perugia
G. Pasquali Fondazione Maugeri, Pavia
T. Malatesta AFaR Ospedale S.Giovanni Calibita
Isola Tiberina, Roma
G. Montanari A. O. S. Gerardo, Monza
G. Zonca Istituto Nazionale Tumori, Milano
G. Benecchi A.O. Maggiore, Parma
S. Broggi Istituto Scientifico San Raffaele, Milano
A. Bufacchi Ospedale Fatebenefratelli, Roma
G. Capelli Azienda Ospedaliera, Cremona
E. Pignoli Istituto Nazionale Tumori, Milano
C. Talamonti Dip. di Fisiopatologia Clinica, Università, Firenze
A.L. Angelini A.O. S Orsola-Malpighi, Bologna
S. Bresciani Ospedale Umberto I, Torino
M. Dominietto A.O. Maggiore della Carità, Novara

A. Ferri	A.O. S.Orsola-Malpighi, Bologna
P. Francescon	A.O. S. Bortolo, Vicenza
E. Gino	Policlinico S.Matteo, Pavia
B. Ghedi	Ospedali Civili, Brescia
G. Loi	A.O. Maggiore della Carità, Novara
S. Maggi	Ospedale Umberto I, Ancona
F. Romani	A.O. S.Orsola-Malpighi, Bologna
G. Scielzo	Ospedale Umberto I, Torino;
M. Schwarz	Ag. Provinciale per la Protonterapia, Trento
G. Guidi	Ospedale di Modena, Modena

Appendix co-Authors

F. Banci Buonamici	Azienda Ospedaliera Careggi, Firenze
L. Begnozzi	S.Giovanni Calibita-Fatebenefratelli, Roma
M. Benassi	Istituto Regina Elena, Roma
M. Bucciolini	Università and INFN, Firenze
A. Bufacchi	S.Giovanni Calibita-Fatebenefratelli, Roma
S. Cora	Ospedale S. Bortolo, Vicenza
S. DelleCanne	S.Giovanni Calibita-Fatebenefratelli, Roma
M. Donetti	Fondazione CNAO Milano ed INFN Torino
G. Cuttone	LNS - INFN, Catania
E. Garelli	ASP and INFN, Torino
C. Garibaldi	Istituto Europeo di Oncologia, Milano
S. Giordanengo	INFN, Torino;
M. Iori	Arcispedale S. Maria Nuova, Reggio Emilia
E. Madon	OIRM S. Anna, Torino
T. Malatesta	S.Giovanni Calibita-Fatebenefratelli, Roma
F. Marchetto,	INFN, Torino
S. Marzi,	Istituto Regina Elena, Roma
R. Nigro,	Arcispedale S. Maria Nuova, Reggio Emilia
M. Paiusco,	Arcispedale S. Maria Nuova, Reggio Emilia
I.V. Patti	REM Radioterapia and LNS-INFN, Catania
C. Peroni	Università and INFN, Torino
M.G. Sabini	LNS - INFN e REM Radioterapia, Catania
A. Sardo	OIRM S. Anna, Torino
M. Stasi	Istituto per la Ricerca e Cura del Cancro, Candiolo
L.M. Valastro	LNS – INFN, Catania

INDEX

Summary

<i>i</i> <i>Introduzione</i>	pag. 5
<i>ii</i> <i>Introduction</i>	“ 6
<i>iii</i> <i>Structure of the AIFM - IMRT working groups</i>	“ 7
<i>References</i>	“ 9

1. Intensity modulated radiotherapy: definitions and dosimetrical aspects

1.0 Sommario	“ 10
1.1 The IMRT definition.....	“ 10
1.2 IMRT delivery techniques	“ 11
1.3 Basic requirements for IMRT implementation	“ 15
1.4 General dosimetric issues	“ 15
1.5 Dosimetric issues: differences among IMRT techniques.....	“ 17
References	“ 18

2. Commissioning of an IMRT system

2.0 Sommario	“ 20
2.1 Introduction	“ 21
2.2 IMRT delivery system	
2.2.1 Physical and dosimetric characteristics of MLC	“ 22
2.2.1.1 Transmission leakage	“ 22
2.2.1.2 Penumbra	“ 23
2.2.1.3 Tongue and groove effect	“ 23
2.2.2 Delivery system performances	
2.2.2.1 MLC calibration	“ 24
2.2.2.2 Control system of IMRT delivery	“ 24
2.2.2.3 Leaf positioning accuracy	“ 26
2.2.2.4 Leaf speed stability	“ 28
2.2.2.5 Linac performance for small MUs delivery	“ 29

2.3 IMRT treatment planning	
2.3.1 Measurements and preliminary verifications	pag. 30
2.3.2 Commissioning an IMRT treatment planning system	“ 33
References	“ 36

3. Pre-clinical Dosimetry of IMRT treatments

3.0 Sommario	“ 39
3.1 Introduction	“ 41
3.2 Procedures	“ 42
3.3 Film dosimetry	“ 46
3.4 Detector arrays	“ 50
3.5 EPID dosimetry	“ 51
3.6 Parameters to be compared	“ 53

Appendix : Real time 2D verification tools for IMRT

a.0 Sommario	“ 57
a.1 Introduction.....	“ 58
a.2 2D verification systems	
a.2.1 PTW 2D-Array	“ 58
a.2.2 Sun Nuclear MapCHECK (MPC).....	“ 59
a.2.3 Torino University INFN Pixel Ionization Chamber (PXC)	“ 59
a.3 Accelerators, multiLeaf Collimators, Treatment Planning Systems	“ 59
a.4 Results and discussion	“ 60
a.5 Conclusions.....	“ 63
References	“ 65

4. Dose calculation and plan optimisation: computational and radiobiological aspects in IMRT

4.0 Sommario	“ 69
4.1 Introduction	“ 70
4.2 Dose calculation algorithms for IMRT	“ 71
4.3 Monte Carlo algorithms in IMRT: some features.....	“ 73

4.4 IMRT optimisation	Pag. 74
4.5 Cost function definition.....	“ 75
4.6 Minimization: a search for the best treatment plan	“ 77
4.7 Radiobiological Modelling in IMRT	“ 78
4.7.1 Biological conformality	“ 79
4.7.2 Biological objective functions	“ 81
References	“ 83

i. INTRODUZIONE

Nell'ultimo decennio la Radioterapia, quella branca della Medicina che si dedica alla cura dei tumori utilizzando le radiazioni ionizzanti, ha subito un processo di innovazione e di sviluppo tecnologico così rapido e profondo, da ampliare sensibilmente il livello di conoscenza e di competenze richiesto agli operatori del settore. Tra i professionisti direttamente coinvolti nel processo radioterapico, trova collocazione la figura del Fisico Medico che, in qualità di specialista esperto in Fisica Medica, ed in stretta collaborazione con il Medico Radioterapista, responsabile clinico del trattamento, predispone le procedure per l'ottimizzazione e la valutazione delle dosi somministrate ai pazienti, contribuendo a verificarne la corretta applicazione

Numerosi sono i dispositivi e le nuove apparecchiature introdotte clinicamente nei Servizi di Radioterapia, e molte le problematiche inerenti la Fisica, la Dosimetria, l'Assicurazione di Qualità, l'Imaging Multimodale, il Calcolo e la Modellistica Radiobiologica che i Fisici Medici si sono trovati ad affrontare nel corso di pochi anni. Dalle terapie conformazionali (3D-CRT), che sono state introdotte agli inizi degli anni novanta e che sono considerate il gold standard della Radioterapia, si è passati a tecniche di trattamento con fascio modulato (IMRT), attivate clinicamente in Italia agli inizi del 2001, significativamente più complesse ed onerose della 3D-CRT, per poi arrivare in un prossimo futuro a terapie radianti guidate dall'immagine (IGRT). A questo proposito è bene sottolineare che se ad oggi, solo un numero limitato di centri di radioterapia italiani abbia attivato tecniche di IMRT in modalità clinica, seppur queste rappresentino la normale evoluzione della 3D-CRT, questo si deve principalmente al maggior impegno di risorse, stimato il doppio o triplo rispetto alla 3D-CRT [0.1], necessario per attivare e mantenere in uso clinico queste modalità.

In un tale scenario è facile comprendere come l'Associazione Italiana di Fisica Medica (AIFM), cioè l'associazione dei Fisici operanti nel campo della Medicina e della Biologia, abbia sentito l'esigenza di istituire un gruppo di studio che si occupasse delle problematiche inerenti le tecniche speciali di radioterapia conformazionale (3D-CRT), ed in particolare della IMRT. Con questo obiettivo, e su mandato dell'Associazione, si è costituito nel Gennaio del 2002 il I° gruppo di lavoro AIFM-IMRT, che ha visto coinvolti quei Centri ospedalieri nei quali erano già eseguiti trattamenti con fasci modulati, o che erano in fase avanzata di caratterizzazione della metodica. I lavori del gruppo sono stati convogliati in un primo Report dal titolo "Elementi di radioterapia con modulazione d'intensità (IMRT)" pubblicato

nella rivista dell'Associazione "Fisica in Medicina" [0.11].

Valutato il crescente interesse della comunità dei Fisici Medici italiani sull'argomento, ed al fine di accrescere la diffusione in campo clinico delle IMRT, ben sapendo che l'attività espletata dal I° gruppo di studio non poteva considerarsi esaustiva degli aspetti connessi alla modulazione d'intensità, e consapevoli della necessità di realizzare una linea guida preliminare sull'attivazione delle metodiche con fasci modulati, l'AIFM ha ritenuto opportuno attivare un secondo gruppo di studio sull'argomento, costituitosi nel Gennaio 2003. Dal lavoro di questo II° gruppo nasce il Report qui presentato: "*Linee guida italiane sugli aspetti fisici e dosimetrici della modulazione d'intensità*". Per i continui cambiamenti ed i rapidi sviluppi a cui è sottoposta, questo secondo Report AIFM non ha la pretesa di considerarsi un documento definitivo sulla IMRT, ma si propone, nella prima parte, come una linea guida preliminare con la quale confrontarsi per attivare e validare dosimetricamente la metodica, mentre nella seconda parte fornisce alcuni elementi relativi all'Imaging Multimodale, alla Modellistica Computazionale ed alla Modellizzazione Radiobiologica, che costituiscono parte integrante dell'utilizzo dell'IMRT stesso ed in generale delle tecniche innovative in Radioterapia. In particolare questi ultimi sono indicativi della necessità di un più ampio coinvolgimento scientifico, a carattere interdisciplinare, con aree di conoscenza diverse dalla Fisica e quindi anche con le associazioni di professionisti medico-sanitari (AIRO, AITRO, AIMN, SIRM, ...) coinvolti nel campo della radioterapia a modulazione d'intensità.

ii. INTRODUCTION

Over the last decades Radiation Oncology, the branch of Medicine dedicated to the treatment of tumors with ionizing radiation, has changed a great deal, undergoing an innovation and technical development that it considerably widens the level of knowledge and expertise required by the specialist involved in this field. Numerous devices and new equipment have been introduced clinically into the Radiotherapy Department, and there are many problems related to the physics, dosimetry, quality assurance, radiobiological modeling, multi-modality imaging and the informative-technology that physicists, in terms of their expertise in medical physics, have been facing and solving in recent years.

There has been an evolution from conformal radiotherapy techniques (3D-CRT), that were introduced at the beginning of the nineties and are now considered the gold standard in this field, through advanced modalities like intensity-modulated radiation therapy (IMRT), clinically introduced in Italy

at the beginning of 2001, to the image-guided radiotherapy (IGRT) of the near future, this will require further effort both in terms of competence and of human resources, because it is significantly more complex, onerous and time-consuming than 3D-CRT. We should bear in mind that the main reason that IMRT treatments are not yet applied by all Italian Radiotherapy Centers, is that the demand for special treatment unit commissioning, planning and pre-clinical verification procedures, with an estimated factor of 2 - 3 [0.1] compared to 1 3D-CRT modalities, have restricted its clinical introduction.

Given this situation easy to understand why the Italian Association of Medical Physics (AIFM), the scientific society for physicists working in the medical and biological and Biology fields, asked that a working committee on the newer radiotherapy techniques, be set up. Its task was to give some preliminary indications on IMRT techniques, making reference to all the reports already published in the Literature on 3D-CRT [0.2], and to the documents prepared by the AIFM on Brachytherapy [0.3] and by the Italian National Institute of Health (ISS, www.iss.it) on 3D-CRT [0.4, 0.5, 0.6, 0.7], on Brachytherapy [0.8], on Intra-Surgery Radio-Therapy (IORT) [0.9] and on Total-Body Irradiation [0.10].

iii. Structure of the AIFM - IMRT working groups

In January 2001 the first AIFM-IMRT committee was constituted, involving physicists working in hospitals where IMRT treatments were already carried out or were in an advanced state of commissioning. The activity of that working group was focused towards an in-depth revision of the scientific literature, making an attempt to describe the principal characteristics of IMRT technology, dosimetry and inverse planning, and to identify the more critical aspects related to IMRT device commissioning. All these reflections, in the light of Italian expertise at the time, formed a first AIFM report called "Elements on Radiotherapy with Intensity Modulation (IMRT)". This report, drawn up only in the Italian language, was published in 2003, in the AIFM (www.aifm.it) journal "Fisica in Medicina" [0.11]. Since that report was written, other Radiotherapy Departments in Italy have moved towards the dosimetric characterization and/or the clinical activation of intensity-modulated techniques. Only a small number of hospitals were involved in this early period. The experience of intensity modulation on the part of Italian centers has now increased to the point that we can start thinking about drawing common, shared AIFM guidelines on IMRT. In addition, following the preliminary RTOG guidelines [0.12] on IMRT, many Medical Physicists in Italy were struggling with the question "what do I need to know and to do in order

to implement IMRT safely and effectively”.

To promote the learning of IMRT techniques, and contribute to its more rapid clinical spreading, in the year 2003 a second AIFM committee was constituted. This time the committee’s tasks were to prepare preliminary Italian guidelines on the physical aspects of IMRT, and to review additional aspects common to complex radiotherapy treatments, and in particular to IMRT modalities. Seven sub-commissions have prepared the material discussed in this two-party report, trying to avoid repetition of the already published documents [0.13, 0.14, 0.15].

Because of the emerging and rapidly changing nature of IMRT and of all other aspects connected with it, the actual report should be considered only as a preliminary guideline for this subject, bearing in mind that information and more detailed codes of practice will certainly emerge as these fields of radiotherapy become more mature. The present report is drawing entirely in the English language, and to allow a wider text description, each chapter is preceded by a short abstract in Italian. The framework of the report is organized in this way:

1. Intensity modulated radiotherapy: definitions and dosimetrical aspects.

This paragraph proposes a synthetic definition of the principal IMRT modalities with a short description of the specific characteristics for each technique.

2. Commissioning of an IMRT system.

This paragraph proposes some specific and widely employed procedures for the dosimetric characterization and activation of an IMRT system, composed of an inverse-planning module and dynamic MLC devices

3. Pre-clinical dosimetry of IMRT treatments.

This paragraph deals with patient quality assurance procedures when the modulation techniques are employed and more generally describes pre-clinical dosimetry verifications. *Appendix* : presents the preliminary results of a simplified dosimetric comparison realized with different 2D matrix detectors in some Italian Centers.

4. Dose calculation and plan optimization: computational and radiobiological aspects in IMRT.

In this paragraph, the basic structures of an inverse-planning module together with the principal limitations and critical points of the calculation algorithms and optimization process are described.

Moreover, this paragraph deals with both radiobiological modeling and common indicators generally used to evaluate treatment plans with highly non-homogeneous dose-distributions.

The preliminary work of this committee was already published, in its draft form, as an ISTISAN report [0.16] in Italian by the National Health Institute (ISS).

References

01. Policy Statement of the Institute of Physics & Engineering in Medicine IPeM, "Guidelines for the provision of a physics service to radiotherapy" York, UK; 2002.
02. Z Kolitsi, O Dahl, R Van Loon, J Drouard, J Van Dijk, BI Ruden, G Chierego and JC Rosenwald "Quality assurance in conformal radiotherapy: DYNARAD consensus reports on practice guidelines" *Radiother Oncol* 45: 217-223; 1997.
03. AIFM report, "Dosimetric problems in the new brachytherapy techniques" 2003 (in Italian).
04. ISTISAN report 99/06, "Minimal requirements for quality controls in radiotherapy with external beams" 1999 (in Italian).
05. ISTISAN report 00/29, "Quality controls in radiotherapy" 2000 (in Italian).
06. ISTISAN report 02/15, "Dosimetry inter-comparisons for high-energy photon beams" 2002 (in Italian).
07. ISTISAN report 04/34, "Indications for quality assurance in conformal radiotherapy in Italy" 2004 (in Italian).
08. ISTISAN report 99/04, "Quality Assurance in brachytherapy: proposal of guidelines concerning clinical, technological and physical-dosimetry aspects" 1999 (in Italian).
09. ISTISAN report 03/1, "Guidelines for intra-operative radiation therapy" 2003.
010. ISTISAN report 02/39, "Guidelines on quality assurance in total body irradiation" 2002 (in Italian).
011. AIFM report, "Elementi di IMRT" *Fisica in Medicina* 1,2,3,4; 2003 (in Italian).
012. Preliminary report of IMRT subcommittee of the Radiation Therapy Oncology Group (RTOG), "Guidance document on Delivery, Treatment Planning, and Clinical Implementation of IMRT" 2004.
013. Intensity Modulated Radiation Therapy Collaborative Working Group "Intensity-modulated radiotherapy: current status and issues of interest" *Int J Radiation Oncology Biol Phys* 51: 880-914; 2001.
014. JM Galvin, G Ezzell, A Eisbrauch, C Yu, B Butler, Y Xiao, I Rosen, J Rosenman, M Sharpe, L Xing, P Xia, T Lomax, DA Low and J Palta "Implementing IMRT in clinical practice: a joint document of the American Society for Therapeutic Radiology and Oncology and the American Association of Physicists in Medicine" *Int J Radiation Oncology Biol Phys* 58: 1616-1634; 2004.
015. The National Cancer Institute Guidelines for the Use of Intensity-Modulated Radiation Therapy in Clinical Trials. Department of Health and Human Services, 14 January 2005, Bethesda, Maryland (www.cancer.gov/trp/).
016. ISTISAN report 05/14, "Strumenti di lavoro in radioterapia con fasci ad intensità modulata" 2005 (in Italian).

1. The intensity modulated radiotherapy: definitions and dosimetical aspects

1.0 Sommario

Nel presente capitolo vengono messe in evidenza le caratteristiche peculiari della tecnica di radioterapia ad intensità modulata (IMRT), considerata generalmente una forma evoluta della radioterapia conformazionale 3D. Vengono descritte in modo sintetico le tecniche utilizzate per realizzare la modulazione dell'intensità del fascio di radiazioni mettendo in evidenza soprattutto le differenze sostanziali fra le tecniche stesse. Una prima distinzione viene fatta tra le modalità di erogazione a gantry fisso e gantry rotante; un'ulteriore distinzione viene fatta tra la tecnica statica e quella dinamica nell'utilizzo del collimatore multilamellare (MLC), mentre tra le tecniche rotazionali viene definita la tecnica ad intensità modulata con arco (IMAT) mettendo in evidenza la sua differenza con quella conformazionale ad arco. La Tomoterapia seriale ed elicoidale (ST e HT IMRTs) insieme alla macchina CyberKnife completano il quadro generale delle tecniche e delle apparecchiature dedicate alla modulazione di intensità attualmente disponibili sul mercato.

Viene indicata la dotazione essenziale per un utilizzo clinico della metodica IMRT e sono considerati alcuni aspetti dosimetrici generali comuni a tutte le tecniche IMRT che consentono di ottenere indici di conformazione superiori alle tecniche tradizionali conformazionali, tenendo presente anche della maggiore criticità intrinseca di questa metodica.

Sempre riguardo agli aspetti dosimetrici sono messe in evidenza le differenze sostanziali fra le varie tecniche e le eventuali limitazioni pratiche nella loro esecuzione.

1.1 IMRT definitions

The Intensity Modulated Radiation Therapy (IMRT) definitions available in the literature reports or publications, generally agree to focus their attentions on these two characteristic aspects: the first one concerns the modalities to deliver intensity-modulation, the second one is connected with the achievable dose distribution produced by fluence modulation [1.1, 1.2, 1.3]. Both these characteristics can be generally summarised as follows:

- the IMRT can be seen as an evolution of three-dimensional conformal radiotherapy (3DCRT), which adds to the geometric shaping of the beam (conformal therapy) a modulation of the beam fluence [1.1, 1.2,

1.3, 1.4]. These non-uniform radiation fluencies, historically indicated as intensity-modulation, are generally obtained by specific treatment planning software called “inverse planning” [1.1]. The planner specifies beam directions (or arc angle), dose or dose-volume constraints for the target and sensitive structures (OARs) and the optimisation algorithm calculates the intensity patterns (fluence maps) that create the dose distribution that best satisfies constraint prescriptions.

- the main difference between IMRT and other 3-D conformal techniques lies in the possibility to obtain concave-shaped dose distributions [1.1]. Thus it is possible to conform the higher doses to complex target volumes, and, at the same time to spare the more sensitive structure in the close proximity of the target (conformal avoidance) [1.22, 1.4].

1.2 IMRT delivery techniques

The delivery modalities of IMRT techniques can be generally divided in two main classes:

1. **Fixed-gantry:** the beam direction is constant during the modulation of the beam fluence;
2. **Rotating-gantry (or dynamic gantry):** the gantry moves during the irradiation, and the collimator shape and gantry angle are indexed to the delivered dose.

Physically, a common feature of these IMRT techniques is that they allow to achieve a higher conformal three-dimensional dose distribution through the superposition of a large number of independent segmented fields from either a number of fixed directions or from multiple directions distributed along one or more arcs.

Generally if the multi-leaf collimator (MLC) leaves or the MLC plus the gantry move when the beam is turned on, the delivery is referred to as dynamic. In Figure 1 a schematic diagram of the IMRT techniques is reported [1.34].

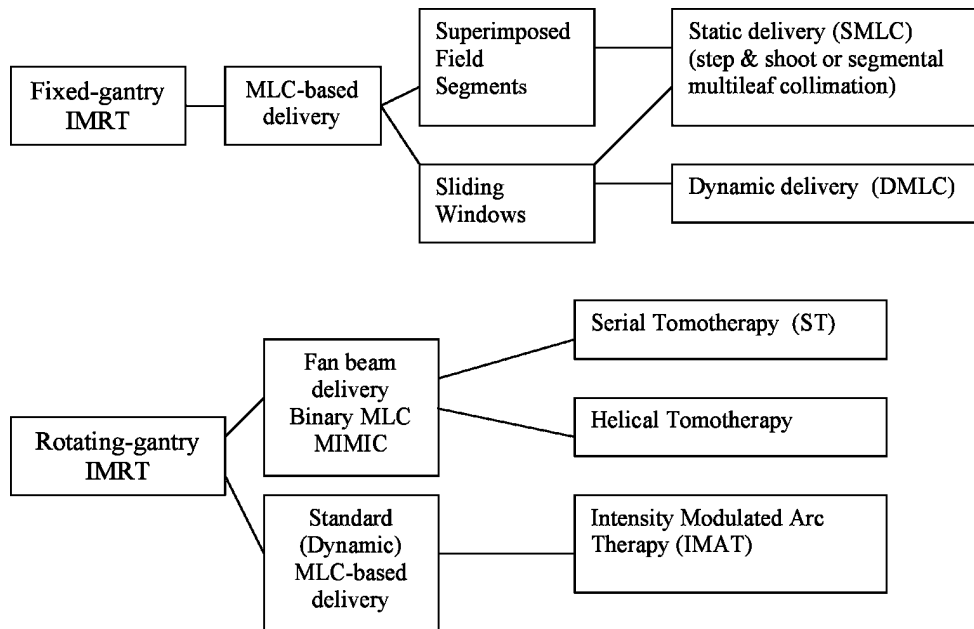


Fig. 1. IMRT techniques schematic diagram

1. The **Fixed-gantry class** includes the delivery techniques which employ a conventional multileaf collimator (MLC) either in static (SMLC-IMRT) or in dynamic mode (DMLC-IMRT) and the use of compensating filters.

In the **static delivery**, for each beam direction, the fluence modulation is obtained delivering a sequence of static MLC-shaped sub-field or segments, each with a uniform fluence: the collimator shape does not change during irradiation but it changes between consecutive sub-fields. The desired intensity pattern is obtained by the fractional weighted summation of the intensity patterns from all subfields. The monitor units are calculated for each sub-field, at the end of the inverse planning and sequencing processes. After delivering each subfield, the accelerator is turned off, the leaves move to define the next sub-field and the accelerator is turned on again. The number of fields generally used in the static IMRT technique, varies from five to nine. The number of subfields required for each field is related to the complexity of the intensity map. Generally, more complex are the fluence patterns calculated by the inverse-planning system, higher is the number of subfields defined by the MLC sequencer to deliver the plan.

The **dynamic delivery** differs from the static technique because the collimator shape changes during irradiation, that means that the leaves move from

one configuration to the following one while the beam is on, while the gantry is fixed. Each pair of leaves of the MLC, defining a gap, moves generally unidirectionally (sliding window modality) during the irradiation and each leaf travels with an independent velocity as a function of time.

In the dynamic technique, all leaves are motor driven, capable of a high leaf speed, generally greater than 2 - 2.5 cm/s, and the linac is equipped with a system to accurately monitor the positions of the leaves during their motion at regular intervals. Varying the sizes of the gaps defined by the leaves, as well as the times the gaps remain open (dwell times) allows a variable intensity to be delivered to each point of the treatment field. In the sliding window technique the leaves change their speed between different segments while they keep a constant speed during a segment. During their motion, one leaf of each pair travels with its maximum speed, compatible with the modulation, in order to minimise the beam-on time. Since not all leaf pairs finish their motion at the same time, the time required to complete the treatment field is equal to the time required by the slowest leaf pair to travel along the entire field.

A more exhaustive description, of how the fluence modulation of photon beams is produced by dynamic MLC devices, together with a wide view on the technical characteristics of all MLCs, is available on the first AIFM report on IMRT [1.23]. For those who are interested to investigate the IMRT techniques in more detail, these publications are advisable [1.24, 1.25].

2. The **Rotating-gantry class** includes all techniques delivered with the rotation of the gantry while the beam is on. The most important are the **Serial Tomotherapy** (ST), the **Helical Tomotherapy** (HT-IMRTs) (with rotating fan beams), and the **Intensity Modulated Arc Therapy** (IMAT). [1.17]

The **Serial Tomotherapy** has been the first IMRT rotational technique to be developed (NOMOS Corporation, US) and clinically implemented. The modulation of beam intensity is obtained through a binary-intensity rotational slit beam, (MIMiC, Multileaf Intensity Modulation Collimator) (20 leaves, dimensions 20 cm in diameter and 2 to 4 cm in the longitudinal direction) which is used to successively treat thin slices of the target volume. Each slice of the treatment field is irradiated with temporally modulated fan beams that typically rotate in 270°-300° arcs around the patient. The intensity at any moment is controlled by leaf shutters, which are driven in and out of the path of radiation, according to a pattern indicated by intensity optimisation methods. The movement of the treatment couch is coupled with gantry rotation

and the couch is stopped during irradiation. The Serial Tomotherapy has its own treatment planning system with inverse planning capabilities.

A new machine developed by TomoTherapy is able to move the treatment couch during the irradiation for **Helical Tomotherapy**. The TomoTherapy system consists of the following completely integrated components: a rotating gantry assembly, upon which the linear accelerator (6 MV) and CT detector subsystems are mounted. The collimator is similar to MIMiC and has dimensions 5 x 40 cm² with 64 leaves (leaf width 6.25 mm) [1.31, 1.32]. Using the accelerator beam with a reduced energy, it is possible to acquire Mega Voltage (MV) CT images for patient positioning verification, leading to image-guided treatments (IGRT). The Tomotherapy is equipped with a dedicated inverse planning system for the treatment plan optimisation.

Another rotational technique was first proposed by Yu [1.12] and defined as **IMAT** (Intensity Modulated Arc Therapy): employing a conventional accelerator and a standard MLC, it combines gantry rotation and dynamic multileaf collimation. During arc delivery, the field shape defined by the MLC changes continuously and intensity modulation is achieved by multiple overlapping arcs, each arc having a different set of field shapes and, typically, different weights (that is, different rotation speeds). In an IMAT treatment, the beam openings defined by MLC do not cover the entire PTV for the whole treatment, as in conventional conformal dynamic arc treatments. In the following clinical implementations [1.5, 1.6, 1.13, 1.14, 1.30] arc modulation techniques are simplified with respect to the original study proposed by Yu [1.12] using a forward planning. The subfields shapes are not based on intensity maps calculated by an inverse planning software, but are generally derived directly by the user from the BEV projections of the PTV and OARs: during gantry rotation using automatic shaping tools, the MLC either conforms on the whole BEV of the PTV, or excludes those PTV regions which overlap with OARs.

At the moment, complete inverse planning dedicated to the optimization of IMAT-like treatments are not commercially available, and this must be kept in mind when evaluating the actual capability of this modulation technique. Anyway, some systems [1.10] offer the possibility to optimize, using an inverse planning software, the weights of the arcs already defined by the user, and in the literature some inverse planning modules for IMAT, even if as research prototypes, start to appear [1.15].

A new device, which adopts a delivery technique substantially different from those described above, any way able to produce dose distributions sim-

ilar to those obtained by IMRT treatments, is the *CyberKnife*. Developed by Accuray [1.18] for stereotactic radiosurgery, this system consists of a compact 6 MV linear accelerator equipped with 12 cylindrical collimator and assembled on a computer controlled robotic arm with six degrees of freedom, an x-ray positioning control system and a dedicated treatment planning system with inverse planning capabilities. The system uses a predefined set of positions (100) on the surface of a virtual sphere; from each position the beam axis can be oriented along 12 possible directions, for a total of 1200 different usable trajectories during the treatment.

1.3 Basic requirements for IMRT implementation

All fore mentioned techniques (except for Cyberknife), make use of a multileaf collimator. In addition, treatment planning systems need generally an Inverse Planning (even if a forward planning can be used) software and a sequencer. The sequencer translates the optimal fluence density matrix computed by the inverse planning module into a real fluence map deliverable by the MLC. It takes into account the limitations in the leaf movements (leaf speed) and the MLC transmission factor (mean value between intra- and inter-leaf leakage). Best results seem achievable when the sequencer is incorporated in the optimisation process and not applied after it as separate tool [1.19, 1.20].

The algorithms implemented and actually used in the treatment planning system may have a large impact on dose distribution calculation and optimisation, mainly when considering inhomogeneity correction (primary beam fluence and scattered radiation) and secondary electron transport calculation, whose effect increases with decreasing beam dimensions. To this purpose the relevant issues that should be considered are:

- whether the correction algorithm is applied during the optimisation process or only at its end;
- what degree of accuracy is achievable in Monitor Unit (MU) calculation as beam dimensions decrease.

1.4 General dosimetric issues

The better dose conformation achievable by IMRT techniques compared to 3-D conformal radiotherapy can be explained by the following items:

- the greater number of degrees of freedom available to obtain complex dose distributions tightly conformed to target volumes of irregular shape, while exposing less normal tissue volume to high doses;

- the feasibility of partial compensation of beam penumbra, so reducing beam dimension, by fluence increase at target edges;
- reduced influence of beam incidence on dose distribution, allowing a more suitable modelling of low doses around critical organs.

A further opportunity offered by IMRT is the capability of modifying dose gradients and their positions within the irradiated volume, thus allowing the simultaneous deliver (in the same treatment session) of a certain dose to the gross tumour volume (GTV) and a lower dose to the regions of sub-clinical involvement (CTV) or elective irradiation. The advantage of this treatment strategy (Simultaneous Integrated Boost – SIB) consists in the ability of achieving dose conformity indexes much higher than those obtained by conformal therapies and in a radiobiological advantage compared to the sequential boost strategy [1.7, 1.8].

In IMRT treatment planning special care must be paid to evaluate the dose inhomogeneity within the target volume; as a general rule it increases when:

- an increased dose difference is demanded between target and adjoining organs at risk;
- the distance between target and structure at risk decreases;
- a greater concavity is required in dose distribution;
- the number of employed beams is reduced.

Therefore, if the pursued objective is to obtain a concave dose distribution around a complex target volume, whose position is in the close proximity of critical organs, the dose inhomogeneities within the target volume is a consequence that can't be generally avoided [1.1].

One of the most important aspects to be considered, when IMRT techniques are used, is the chance that the target volume may not be adequately covered by the planned dose distribution, during all the treatment-session time. This effect could lead to a partial under dosage of the tumour, or an over dosage of the surrounding healthy tissue due to the presence of high dose gradients in the beams, in both cases frustrating/aggravating the treatment outcome. In IMRT treatments these problems are much more critical than in 3D-CRT, and this is usually due to:

- organ movements or volume changes (deformations) during treatment;
- patient movements;
- patient set-up errors.

The outcome of an IMRT treatment is therefore largely dependent on the

fore mentioned problems that need a thorough analysis enabling the choice of the most appropriate devices and techniques to bring such drawbacks within acceptable limits.

The evolution of IGRT (image guided radiation therapy) techniques (like for instance, cone-beam CT devices mounted on a standard linac [1.26, 1.27]), together with the recent development of devices that synchronise beam deliver and respiratory phases [1.28], will enable the extension of IMRT techniques also to those anatomic regions where the advantages of a better dose distribution could be frustrated by set-up inaccuracy or internal organ movements/deformations (lung, prostate, etc.).

1.5 Dosimetric issues: differences among IMRT techniques

All the different IMRT techniques (SMLC, DMLC, IMAT, ST, HT) can in theory be applied to the same tumour types, even if each of them could have its own specificities related to a particular anatomical district or complex-tumour shape. These specificities are defined in terms of overall MU number (integral dose to the body), beam-on time, whole treatment delivery time, conformation level on target volumes, achievable dose sparing of the healthy tissues surrounding the PTV [1.11, 1.31].

When complex tumour volumes must be treated, and many intensity-modulated beams are used, the duration of a single IMRT treatment session is generally longer than conventional conformal treatments. In these cases, the radiobiological problems, connected to the sub lethal damage recovery during each treatment session, should require more attention [1.21, 1.8, 1.9]. Furthermore, it should be remembered that the dose-bath resulting from a rotational therapy is a still open subject in term of radiobiology comprehension [1.3, 1.9, 1.29].

The IMRT techniques are also used when the capabilities of fluence modulation (Intensity-Modulated RadioSurgery - IMRS) must be added to stereotactic characteristics [1.16, 1.32, 1.33] to improve the final treatment efficacy.

However, it is necessary to emphasise that in the literature there are only few studies comparing the different IMRT techniques, especially fixed-gantry techniques versus rotational techniques. Therefore, it is difficult today to draw precise and definitive conclusions on the real advantages and limitations of each single intensity-modulated treatment modality [1.9, 1.5, 1.29, 1.34, 1.35].

References

- 1.1 *Intensity Modulated Radiation Therapy Collaborative Working Group. Intensity-Modulated Radiotherapy: current status and issues of interest.* Int J Radiation Oncology Biol Phys 51: 880-914; 2001.
- 1.2 "Guidance document on delivery, treatment planning, and clinical implementation of IMRT: Report of the IMRT subcommittee of the AAPM radiation therapy committee." Med Phys 30: 2089-2114; 2003.
- 1.3 "Intensity modulated radiation therapy: A clinical review." C Nutting, DP Dearnalay, S Webb. BJR 73:459-469; 2000
- 1.4 *Intensity Modulated Radiotherapy.* ES Sternick, MP Carol, W. Grant III. Treatment planning in Radiation Oncology (1998) cap. 9.
- 1.5 CX Yu, XA Li, L Ma, D Chen, S Naqvi, D Schepard, M Sarfaraz, TW Holmes, M Suntharalingam, CM Mansfield. "Clinical implementation of intensity-modulated arc therapy". Int J Radiat Oncol Biol Phys 53: 453-463; 2002.
- 1.6 E Wong, JZ Cheen, J Greenland. "Intensity-modulated arc therapy simplified." Int J Radiat Oncol Biol Phys 53: 222-235; 2002
- 1.7 M Oldham and S Webb. "Intensity-modulated radiotherapy by means of static tomotherapy: A planning and verification Study." Med Phys 24 (6), 827-836; 1997.
- 1.8 R Mohan, Q Wu, M Manning, R Schmidt-Ullrich. "Radiobiological considerations in the design of fractionation strategies for intensity modulated radiation therapy of head and neck cancer." Int J Radiat Oncol Biol Phys 46:619-630; 2000.
- 1.9 E Glatstein. "Intensity Modulated Radiation Therapy: The inverse, the converse and per-verse." Seminars in Radiation Oncology V. 12, NO 3, 272-281. July 2002.
- 1.10 R Pellegrini. "AMOA: La modulazione di dose nella tecnica di conformazionale dinamica." Atti del congresso "Radioterapia a modulazione di intensità: dalla fisica alla clinica". Bormio, 2000.
- 1.11 CS Chui, FC Maria, E Yorke, S Spirou, and CC Ling. "Delivery of intensity-modulated radiation therapy with a conventional multileaf collimator: Comparison of dynamic and segmental methods." Med Phys 28(12); 2001.
- 1.12 CX Yu. "Intensity-modulated arc therapy with dynamic multileaf collimation: an alternative to tomotherapy." Phys Med Biol 40: 1435-1449; 1995.
- 1.13 W Duthoy, W De Gerssem, K Vergote, M Coghe, T Boterberg, Y De Deene, C De Wagter, S Van Belle, W De Neve. "Whole abdominopelvic radiotherapy (WAPRT) using intensity-modulated arc therapy (IMAT): first clinical experience." Int J Radiat Oncol Biol Phys 57: 1019-1032; 2003.
- 1.14 M Iori, M Paiusco, A Nahum, P Marini, C Iotti, R Polico, A Venturi, L Armaroli, G Borasi. "IMRT: the Reggio Emilia experience." 7th Biennal ESTRO meeting on physics and radiation technology for clinical radiotherapy. Radiother Oncol 68 (S62); 2003.
- 1.15 MA Earl, Shepard DM, Naqvi S, Li XA and Yu CX. Inverse planning for intensity-modulated arc therapy using direct aperture optimisation. Phys Med Biol 48: 1075-1089; 2003.
- 1.16 FF Yin, S Ryu, M Ajlouni, J Zhu, H Yan, H Guan, K Faber, J Rock, M Abdalhak, L Rogers, M Rosenblum, JH Kim. "A technique of intensity-modulated radiosurgery (IMRS) for spinal tumors." Med Phys 29 (12):2815-22; 2002.
- 1.17 TR Mackie, T Holmes, S Swerdloff, PJ Reckwerdt, JO Deasy, J Yang, B Paliwal, T Kinsella. "Tomotherapy: A new concept for the delivery of dynamic conformal radiotherapy." Med Phys 20: 1709-1719; 1993.

- 1.18 JR Adler, RS Cox. "Preliminary clinical experience with the Cyber-Knife: image guided stereotactic radiosurgery." *Radiosurgery*; 1: 316-326; 1995.
- 1.19 V Jeffrey, V Siebers, M Lauterbach, P J Keall, Radhe Mohan. "Incorporating multi-leaf collimator leaf sequencing into iterative IMRT optimization." *Med Phys* 29 (6); 2002.
- 1.20 DW Litzenberg, JM Moran, BA Fraass. "Incorporation of realistic delivery limitations into dynamic MLC treatment delivery." *Med Phys* 29 (5); 2002.
- 1.21 M Xiangkui, PO Löfroth, M Karlsson, B Zackrisson. "The effect of fraction time in intensity modulated radiotherapy: theoretical and experimental evaluation of an optimisation problem." *Radiother Oncol* 68: 181-187; 2003.
- 1.22 YJ Chen, A Liu, PT Tsai, NL Vora, RD Pezner, TE Schultheiss, JY Wong. "Organ sparing by conformal avoidance intensity-modulated radiation therapy for anal cancer: Dosimetric evaluation of coverage of pelvis and inguinal/femoral nodes." *Int J Radiat Oncol Biol Phys* 63, 274-281; 2005.
- 1.23 AIFM-IMRT committee. *Element of IMRT*. Fisica in Medicina 2003; 1 - 4 (in Italian).
- 1.24 S Webb. "The Physics of Conformal Radiotherapy: advances in technology." IOPP, Bristol: 1997.
- 1.25 S Webb. "Intensity Modulated Radiation Therapy". IOPP, Bristol: 2000.
- 1.26 DA Jaffray, JH Siewerdsen, JW Wong, AA Martinez. "Flat-panel cone-beam computed tomography for image-guided radiation therapy." *Int J Radiat Oncol Biol Phys* 53, 1337-1349; 2002.
- 1.27 J Pouliot, A Bani-Hashemi, J Chen, M Svatos, F Ghelmansarai, M Mitschke, M Aubin, P Xia, O Morin, K Bucci, M Roach, P Hernandez, Z Zheng, D Hristov, L Verhey. "Low-dose megavoltage cone-beam CT for radiation therapy." *Int J Radiat Oncol Biol Phys* 61: 552-560; 2005.
- 1.28 *High-Precision Radiation Therapy of Moving Targets*. Seminars in Radiation Oncology 14 (2004).
- 1.29 P Wieland, B Dobler, S Mai, B Hermann, U Tiefenbacher, V Steil, F Lohr. "IMRT for post-operative treatment of gastric cancer: covering large target volumes in the upper abdomen: a comparison of a step-and-shoot and an arc therapy approach." *Int Journ Oncol Biol Phys* 59: 1236-1244; 2004.
- 1.30 W Duthoy, W De Gerssem, K Vergote, M Coghe, T Boterberg, C De Wagter, C Derie, P Smeets, W De Neve. "Clinical implementation of intensity modulated arc therapy (IMAT) for rectal cancer." *Int J Radiat Oncol Biol Phys* 57: 1019-1032; 2003.
- 1.31 T Kron, G Grigorov, E Yu, S Yartsev, JZ Wong, G Rodrigues, K Trenta, T Coad, G Barman, J Van Dyk. "Planning evaluation of radiotherapy for complex lung cancer cases using helical tomotherapy." *Phys Med Biol* 49: 3675-3690; 2004.
- 1.32 S Yartsev, T Kron, L Cozzi, A Fogliata, G Barman. "Tomotherapy planning of small brain tumours." *Radiother Oncol* 74, 49-52; 2005.
- 1.33 M Fuss, BJ Salter, JL Caron, DG Vollmer, TS Herman. "Intensity-modulated radiosurgery for childhood arteriovenous malformations." *Acta Neurochir* (2005).
- 1.34 JM Galvin, G Ezzell, A Eisbrauch, C Yu, B Butler, Y Xiao, I Rosen, J Roseman M scarpe, L Xing, P, Xia, T Lomax, DA Low, J Palta. "Implementing IMRT in clinical practice: a joint document of the American Society for Therapeutic Radiology and Oncology and American Association of Physicists in Medicine." *Int J Radiat Oncol Biol Phys* 58: 1616-1634; 2004.
- 1.35 L Cozzi, A Fogliata, A Bolsi, G Nicolini, J Bernier. "Three-dimensional conformal vs. intensity-modulated radiotherapy in head-and-neck cancer patients: comparative analysis of dosimetric and technical parameters". *Int J Radiat Oncol Biol Phys*;58 (2): 617-24; 2004.

2. Commissioning of an IMRT system

2.0 Sommario

Il *commissioning* di un sistema IMRT ha come obiettivo la garanzia dell'accuratezza e affidabilità della tecnica attraverso la verifica dei parametri specifici. In questo capitolo verrà fornita una guida ai test, con relativi criteri di accettabilità, essenziali per la validazione del sistema IMRT e saranno proposti alcuni spunti di riflessione e approfondimento. Sebbene non sia sempre facile distinguere la fase di *planning* da quella di erogazione, uno sforzo è stato compiuto dagli autori al fine di individuare alcuni test specifici che possano evidenziare eventuali anomalie del sistema di erogazione e limitazioni del sistema di pianificazione

La modulazione della fluenza, caratteristica peculiare di questa tecnica, è ottenuta, sia per la tecnica a gantry fisso (statica e dinamica) che quella a gantry rotante (IMAT), suddividendo il campo radiante in piccoli segmenti, ognuno dei quali definito dal collimatore multi-lamellare (MLC). La corretta caratterizzazione dei parametri fisico-dosimetrici del MLC costituisce, perciò, il requisito essenziale per l'implementazione della tecnica IMRT. L'accuratezza della dose erogata dipende in modo sensibile dalla trasmissione *inter-leaf* e *intra-leaf*. La misura di tale parametro richiede l'uso di rivelatori ad ampio volume sensibile in modo da ottenere, mediante un corretto campionamento, un valor medio rappresentativo sia della trasmissione *inter-leaf* che *intra-leaf*, unico valore generalmente richiesto dal TPS.

La penombra delle lamelle, nella direzione del moto, deve essere misurata con un rivelatore ad alta risoluzione spaziale per evitare effetti di volume. Il ruolo della penombra è particolarmente critico nelle situazioni in cui sono richiesti elevati gradienti di dose. Inoltre, contrariamente a quanto si verifica in un trattamento conformazionale, i campi a modulazione di intensità, proprio per la loro segmentazione, presentano diverse zone di penombra nella zona del volume bersaglio. Si raccomanda fortemente di eseguire le misure di *commissioning* del TPS utilizzato per IMRT in modo metodologicamente simile a quanto consigliato per un sistema per stereotassia.

Diversi lavori hanno dimostrato, come un'inaccuratezza di posizionamento delle lamelle del MLC possa influenzare notevolmente la dose erogata. Nella modalità *sliding window*, per le piccole dimensioni dei segmenti e per l'importanza dell'accuratezza del gap tra lamelle opposte, la precisione di posizionamento è ancora più critica. L'accuratezza di posizionamento della lamelle risulta critica anche per la tecnica IMAT in cui la posizione delle

lamelle è correlata alla rotazione del gantry. Diversi test sono stati proposti per verificare l'accuratezza di posizionamento, alcuni dei quali possono essere utilizzati in un programma di Controllo di Qualità.

Nella modalità dinamica, l'accuratezza della dose erogata dipende anche dall'accuratezza con cui la velocità delle lamelle viene controllata. Poiché il sistema di controllo può variare sia la velocità delle lamelle che il dose-rate dell'acceleratore per mantenere la corretta relazione posizione delle lamelle – unità monitor, sono stati individuati test che consentono di controllare entrambe le variabili.

Per la verifica dell'accuratezza del calcolo della dose sia assoluta che relativa, si è dapprima considerata la singolarità delle dimensioni dei segmenti. Le approssimazioni di molti algoritmi di calcolo potrebbero non effettuare correttamente il calcolo della dose in quelle situazioni in cui la condizione di equilibrio elettronico non è verificata. Pertanto, si raccomanda di misurare gli output factors dei campi piccoli mediante un rivelatore ad alta risoluzione spaziale.

La completa validazione del TPS richiede, inoltre, la verifica su fantoccio omogeneo di una serie di piani di trattamento a campi multipli (complanari e non), che simulino situazioni geometricamente simili a quelle cliniche. Successivamente, si suggerisce di verificare alcuni piani di trattamento di pazienti opportunamente ricalcolati utilizzando la geometria del fantoccio impiegato per le misure.

L'accuratezza del calcolo della distribuzione della dose deve essere valutata attraverso film dosimetria, dopo aver effettuato una curva di calibrazione. Uno strumento di analisi quantitativa è fornito dalla funzione Gamma che fornisce una misura delle aree o volumi al di fuori di una tolleranza prefissata. La verifica della dose assoluta erogata può, inoltre, essere effettuata mediante una camera a ionizzazione in punti a basso gradiente di dose. Il livello di accuratezza accettabile è fortemente legato al grado di modulazione richiesta e alla patologia in questione. Ci sembra comunque ragionevole pensare che nel caso di regioni a buona uniformità l'accuratezza nell'erogazione della dose dovrebbe essere entro il 3%.

2.1 Introduction

The Commissioning of an IMRT system must address those aspects in treatment delivery and planning which differentiate IMRT from conventional 3D-CRT (3D Conformal RadioTherapy): essentially, the achievement of a non-uniform fluence distribution and the use of an inverse treatment planning

system. Although IMRT planning and delivery are closely related, some efforts have been made to provide tests which may distinguish the different causes of error. When necessary, specific tests for the different IMRT delivery techniques have been considered.

The following chapter describes the fundamental characteristics of the delivery systems together with their effects on the optimization algorithm. The main purpose is to outline practical guidelines for the validation procedures of IMRT planning and delivery and to indicate possible pass-fail criteria.

2.2 IMRT delivery system

2.2.1 Physical and dosimetric characteristics of MLC

The accuracy of dose delivered and the agreement between calculated and measured dose distributions in IMRT techniques, depend upon adequate computation of the physical and dosimetric characteristics of the MLC such as leaf transmission and scatter, rounded leaf tips, tongue and groove design of the leaf.

2.2.1.1 Transmission leakage

The transmission characteristics of the MLC play an important role specially in the case of fixed-gantry IMRT in dynamic modality (DMLC) and for IMAT, than for IMRT delivered in step-and-shoot modality (SMLC). While for dynamic IMRT, treated volumes are shielded by leaves most of the time, for static IMRT, secondary or feedback collimators can be used [2.1, 2.3, 2.5].

Transmission depends on the density of the leaves and, since it may vary between one MLC and another, it is strongly recommended to measure the transmission of each MLC [2.14].

The scatter component contributes about 10% of the radiation leakage through the MLC leaf and varies slightly as a function of its position in the field. The level of MLC scatter is negligible for static IMRT technique but it may become significant in dynamic IMRT.

Furthermore, most of the commercially available MLCs exhibit a leakage of up to 20% between closed opposing leaves, due to the rounded leaf end design and to the minimum gap generally of 0.5 - 0.6 mm between opposed leaves required to avoid collisions.

The transmission and scatter data are important to correctly convert the

theoretical fluence calculated by the optimisation algorithm into a deliverable fluence and to calculate the MLC segments (by leaf sequencer).

Although most treatment planning systems (TPSs) require a single value for these MLC dosimetric characteristics, the delivered dose is very sensitive to intraleaf transmission and interleaf leakage. In order to correctly sample inter- and intra-leaf transmission, the use of a detector with a large sensitive volume, such as films or Farmer ionisation chambers (IC) or flat parallel ionisation chambers are recommended [2.1, 2.14].

Since the TPS takes into account these dosimetric characteristics in an approximated way, for the case of dynamic IMRT the uncertainty on delivered dose increases as the leaf gap decreases.

2.2.1.2 Penumbra

To accurately model the beam penumbra in the TPS, measurement of the beam profiles with a high resolution detector such as a film or a diode is recommended. In some TPSs it is possible to define a parameter to model the beam penumbra profile obtained with the MLC. In any case it is recommended a comparison between calculated and measured penumbra of a diamond shaped field [2.17].

2.2.1.3 Tongue and groove effect

To reduce radiation leakage between adjacent leaves, all commercially available MLCs have a tongue and groove design (Figure 2.1). This design can lead to underdosages around 30 % in a 2 mm wide region. Figure 2.2 shows the tongue and groove effect for a static MLC: two fields with complementary positions of the leaves are delivered on the same film.

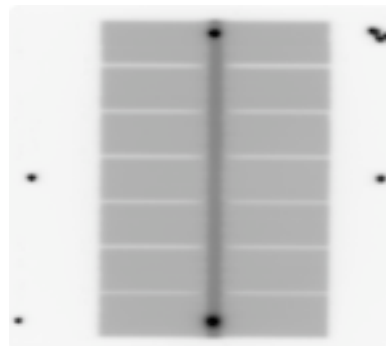
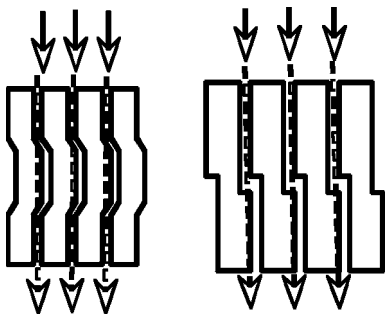


Fig. 2.1 Tongue and groove designs Fig. 2.2 Tongu and groove effect for a static MLC

Most of the inverse planning systems do not consider the tongue and groove effect.

A way to avoid the tongue and groove effect in dynamic delivery is the synchronisation of the movement of adjacent leaf pairs as proposed by Van Santvoort et al [2.33]. The leaf trajectory synchronisation leads to an increased beam-on time, typically of the order of 5% and 15%, causing an increase of radiation leakage.

2.2.2 Delivery system performanc

2.2.2.1 MLC calibration

Most of the commercially available MLCs have a rounded leaf-end design and the leaf motion is linear. With this design, the agreement between the digital MLC position readouts and the light field or radiation field edge must be achieved by using a calibration table in the control system software. For rounded leaf-end design, it is generally not possible to make both the light and radiation field edges agree with the digital readout. Particularly for a dynamic IMRT technique, the MLC leaf calibration must be consistent with the radiation field edge. The maximum difference between the actual radiation field size and the planned field size can be up to 3 mm with a light-field based calibration method. This results in an unacceptable dosimetric error in IMRT treatment. A routine quality assurance testing of the MLC calibration is strongly recommended [2.34].

2.2.2.2 Control system of IMRT delivery

Due to the complexity of IMRT techniques, linac manufacturers have developed MLC control systems that directly control the indexing of the MLC to the delivered monitor units (MU).

In Varian linacs, the control system monitors the leaf positions and compares them to their prescribed positions every 55 ms during dynamic delivery. The beam is momentarily interrupted (beam hold-off) if any leaf position deviates from a tolerance value, generally equal to 2 mm. In theory beam holds-off should never occur if the sequencer correctly takes into account the maximum leaf speed and a specified dose rate while calculating the leaf trajectories. Actually, due to MLC motor fatigue, the effect of acceleration and deceleration and dose rate fluctuations, beam hold-offs can occur. It is therefore recommended that the influence of dynamic leaf tolerance value on the delivery be assessed.

The sequencer's algorithm should incorporate the functionality of the delivery system, like dynamic tolerance, maximum leaf speed and communication delay between the linac control and the DMLC leaf motion control, to improve the accuracy and efficiency of dynamic IMRT treatments. This is not always the case.

For DMLC, when the maximum leaf speed is disregarded by the sequencer and a greater value is necessary to obtain the desired leaf position and MU sequences, the linac control system drives the leaves at their maximum speed while modulating the dose rate according to the following formula:

$$v(\text{cm/s}) = \frac{s(\text{cm}) \cdot \text{dose rate}(\text{MU/min})}{\text{MU}} \cdot 60(\text{s})$$

where “ v ” is the leaf speed and “ s ” is the leaf travel.

In this case, a large number of beam hold-offs occur, in order to reduce them, it is suggested that a low dose rate be used. This kind of dynamic delivery is called “speed-limited delivery”, while it is called “dose rate-limited delivery” if the planned leaf speeds do not exceed the maximum value and the dose rate is constant during delivery. In the case of speed-limited delivery, the resulting intensity profiles may exhibit artefacts when a limited number of MUs are used. An example of speed-limited dynamic delivery is a wedge profile created by a single leaf bank moving at a constant speed greater than the maximum, while modulating the dose rate. The resulting intensity profile is not smooth but exhibits discrete steps [2.3, 2.4, 2.35].

Specific tests should be designed to check delivery conditions that are speed-limited or dose rate-limited. For example, a 1cm wide gap spanning the maximum field width can be programmed. Varying the MUs will regulate the dose rate or the leaf speed. An ionisation chamber set on the central axis will give a reading proportional to the MUs, deviation from that proportionality would be cause concern [2.14, 2.21]

During an IMAT treatment, the leaves move simultaneously with the gantry. Some control systems couple the leaf positions directly to gantry angles [2.10], with others the gantry rotations and the MLC leaf stepping are independently indexed to the delivered MUs [2.8, 2.9, 2.16]. In both cases, the control systems monitor the gantry angles and the corresponding leaf positions and if the dynamic tolerance is exceeded the treatment is either paused or completely stopped [2.8, 2.10, 2.16]. Therefore a careful choice of the tolerance value is important to make the treatment deliverable and accurate. Although values up to 5 mm have been proposed in the literature [2.11],

a 2 mm value seems a reasonable one.

Some MLC controller systems generate a log-file. This file records, at any check time during beam delivery, MLC leaf positions, deviation between actual and planned leaf positions, beam on status and cumulative dose fraction. The log-file can be analysed to verify the accuracy of the delivery system and it is an important tool in checking the long term stability of the system too [2.18]. A detailed analysis of the Varian Dynalog files was carried out by Litzenberg et al [2.36]. Experimental validation of the log-file should become a standard commissioning procedure of a linac for IMRT [2.35].

2.2.2.3 Leaf positioning accuracy

MLC positioning accuracy plays an important role in IMRT treatments [2.2]. A test to check the leaf position accuracy for SMLC is shown in Figure 2.3. It consists of 3 fields of $5 \times 40 \text{ cm}^2$, with the central axis at 0 and $\pm 7.5 \text{ cm}$ off-axis, irradiated on the same film placed at the isocenter. Dose profiles in the direction of leaf movement, evaluated at 50% of the normalised dose, provide information on leaf position and leaf bank alignment (Figure 2.4). The resulting leaf position accuracy is $\pm 1 \text{ mm}$.

Actually the accuracy of the position must be related to the field dimension: Sharpe [2.23] found that a 1 mm deviation from the field size may lead to an output discrepancy of 8% for a $1 \times 1 \text{ cm}^2$ field size.

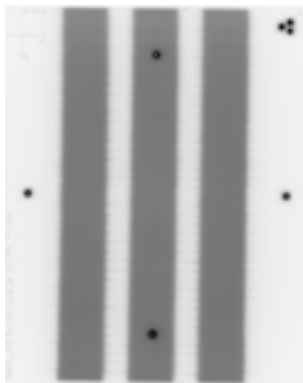


Fig. 2.3 Test to check the leaf position accuracy for SMLC

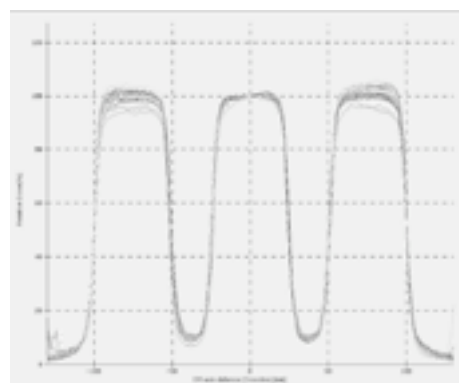


Fig. 2.4 Dose profiles obtained in the direction of leaf movement to evaluate leaf positions and leaf bank alignment

In DMLC the dose delivered is directly related to the gap between opposed leaves as they sweep across the field. As shown in Figure 2.5, the dose error increases with gap error and decreases with the gap width. Therefore, gap width accuracy is essential for DMLC delivery.

Different tests have been proposed to check leaf position accuracy during DMLC commissioning; one of them, suggested by Chui [2.2], consists of a 0.4 x 40 cm² slit beam sweeping across a 20 cm wide field. Each leaf moves at constant speed until it reaches a selected point where it stops for a certain amount of time and then it resumes its motion again. If the leaf positions are accurate and the MLC calibration is correct, the resulting intensity profile, produced on a film, will be uniform, otherwise the stop positions will exhibit hot or cold spots. It is important to constantly check leaf position accuracy in order to keep it always equal or below 0.2 mm.

Another simple test proposed by Chui [2.2] can be used to verify leaf position accuracy daily. The test consists of a sequence that creates 1 mm strips at regular intervals (garden fence). A visual inspection can detect leaf errors with a precision of about 0.5 mm, even if the authors indicate that the test makes it possible to solve a gap discrepancy of 0.2 mm (Figure 2.7).

This test should be performed at different gantry and collimator angles and over the full range of leaf bank motion. A dosimetric analysis of the garden test, performed monthly, provides a quantitative evaluation of leaf position accuracy.

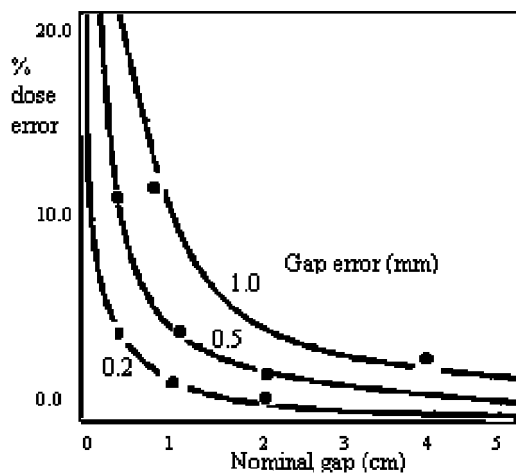


Fig. 2.5 Relationship, for different leaf gaps, between dose-delivery errors and the gap-width errors. Dot points as measured at the Arcispedale S. Maria Nuova

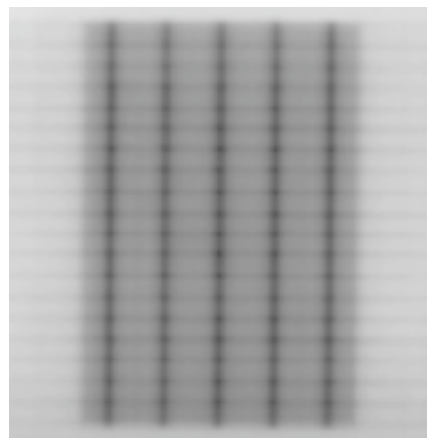


Fig. 2.6 Garden fence test

Tests recommended for DMLC, being performed at a fixed gantry angle, are not suitable for IMAT where the leaf motion is coupled with gantry rotation. The tests already proposed for SMLC are however an essential starting point to check the static leaf position accuracy at fixed gantry angles and the reproducibility of leaf calibration. The tests must be modified by the user to consider the full range of leaf bank motion.

Leaf positioning errors increase with leaf speed both in DMLC and in IMAT delivery techniques. Data for the BrainLAB dynamic micro-multileaf collimator (mMLC) are shown in Figure 2.7 as obtained from the dynalog files created by the mMLC controller.

For IMAT, in order to evaluate the effect of leaf velocity on position error during gantry rotation, Ramsey [2.10] proposes an analysis of the log files of various test plans executed, varying the number of MU and arc-range.

As mentioned before, the influence of gravity on leaf position accuracy has to be assessed [2.1]. For SMLC, the gravity effect on leaf position can be evaluated by checking the light field defined by the MLC at gantry angles of 90° and 270° . The gravity test for the dynamic technique consists of measuring the output of a sliding gap moving at constant speed at different gantry angles by means of an ionisation chamber. The ionisation chamber reading has to be normalised to the reference static field measured at the same gantry angle in order to avoid errors due to an incorrect measuring set-up.

2.2.2.4 Leaf speed stability

The accuracy of DMLC delivery depends also on the accuracy with which the leaf speed is controlled. To verify the stability of leaf speed, individual gaps defined by opposing leaves are created in order to move at different but constant speeds [2.2]. The stability of leaf speed is assured if the delivered intensity profiles are uniform. If the leaf speed is unstable, the resulting intensity profile will show fluctuations greater than 2%, as observed when the maximum leaf speed is used (Figure 2.8).

In some TSPs it is possible to define a maximum value for the leaf speed, usually set lower than the maximum physical speed (i.e. in Helios $v = 2.5$ cm/s and $v_{\max} = 3$ cm/s for Millennium MLC) to assure speed stability and positioning accuracy for clinical fields.

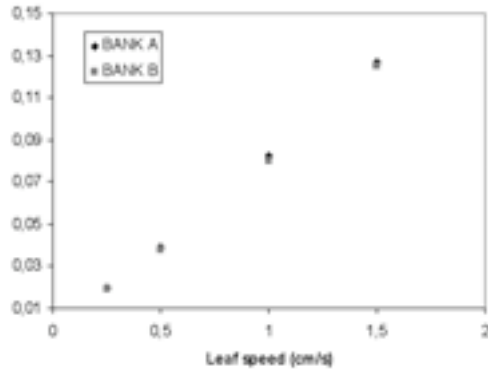


Fig. 2.7 RMS errors in leaf position as a function of leaf speed for the BrainLAB mMLC

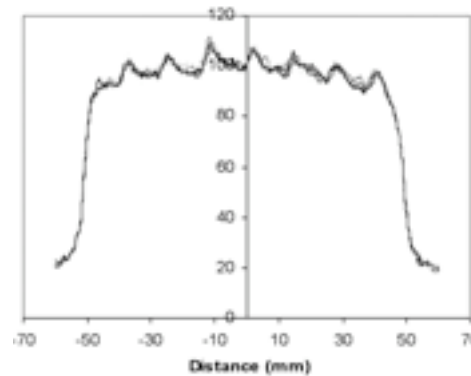


Fig. 2.8 Leaf speed stability test performed at the maximum leaf speed for the BrainLAB mMLC

During the delivery of an intensity-modulated field, the MLC leaves move at different speeds from different segments, they are therefore subject to acceleration and deceleration. To investigate the effect on dose profile, the same test of leaf stability can be performed switching the beam on and off a few times during irradiation [2.2].

2.2.2.5 Linac performance for small MUs delivery

For typical IMRT treatment plans, significant numbers of segments are delivered with monitor units of much less than 10. Verification of the capability of the linear accelerator to accurately deliver small MU segments is an essential step in IMRT commissioning and the quality assurance process. Some authors have reported discrepancies between the planned and the delivered segment MUs in the static MLC technique [2.35, 2.34]. The dose linearity per MU, flatness and symmetry of the beam should be checked [2.28]. An ionisation chamber was used by Sharpe [2.23] and Aspradakis [2.28] to measure the delivered dose as a function of MU values. For a 6 MV beam the deviation of the ionisation reading per MU was found to be within 2% for exposure greater than 4 MU and greater than 2 MU.

The beam profile stability, for small MU and different dose rates, should be checked. A linear array or films have been used to measure symmetry and flatness for small MU values [2.23, 2.28] and good stability for Siemens Primus exposure has been reported for treatment times as short as 1 MU [2.28] and 4 MU [2.23]. These investigations should be done for every energy and for every Linac. It should be remembered that the ability to accurately-

ly deliver small MU segments in the static mode does not guarantee the same accuracy in the dynamic mode. Some authors suggested that the integrity of the linac delivery of small MU should be verified by analysing the log-file created by the control system [2.25].

IMAT, being a rotational technique, requires tests to check the stability of the radiation output with gantry rotation [2.5, 2.6]: the MU linearity should be tested for a variety of gantry arcs that span the clinical range.

2.3 IMRT treatment planning

2.3.1 Measurements and preliminary verifications

The inverse treatment planning commissioning must be connected with the validation of the dose calculation model. This is so for the commissioning of any TPS and neither the optimisation module nor the dynamic MLC delivery system are involved in this process. Accurate modelling of standard static fields does not guarantee that the calculated dose will agree with the delivered one in the case of an intensity modulated beam but it defines attainable accuracy of the dose calculation model.

In order to investigate situations close to the IMRT and IMAT conditions, a check is recommended of depth dose curves and profiles for small fields, also when set in an off-axis position. In SMLC IMRT uniformity should be verified for small fields and minimum MU value allowed. Comparison might be done according to Van Dyk [2.19] or TG53 [2.20] criteria.

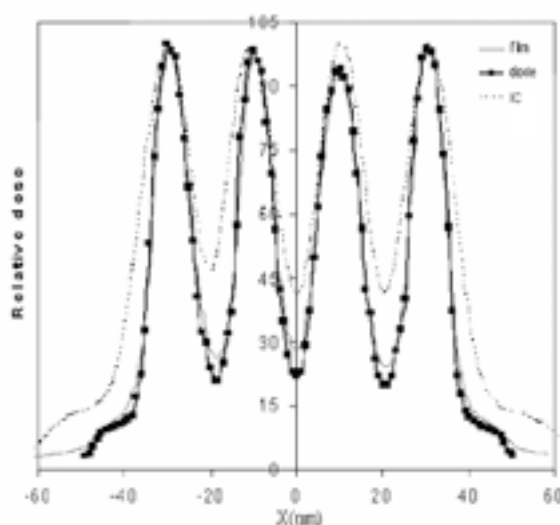


Fig. 2.9 Dose profile measured with film compared with TPS calculation. TPS is commissioned in one case with a diode and in the other with IC RK diameter 0.4 cm

Small fields with highly irregular shapes, present several dosimetric problems. Treatment planning systems make use of dosimetric data acquired under electronic equilibrium and the dose calculations may not be accurate for small irregular segments. For the above reason, the effect on the output factors (OFs) of the loss of lateral equilibrium must be checked. Of great importance is the detector used for measurements, as differences have been found among different detectors [2.26].

For small fields, the secondary electron contribution leads to an overestimation of the OF measured with a non water equivalent diode detector. On the other hand, OFs are underestimated by an IC measurement, probably because of under sampling and lateral electron disequilibrium [2.24, 2.25]. The user must be aware of this in order to avoid using fields that are too small. To solve this dosimetric uncertainty, some TPSs can define the smallest allowed segment size. A small volume (0.015 cm^3) ionisation chamber, the size of a pinpoint, seems to be better than the Farmer chamber, although a diamond detector was found more suitable [2.25].

Small field profiles will supply information about penumbra accuracy. The role of penumbra can be critical in IMRT clinical situations. Unlike conventional conformal fields, IMRT fields have multiple beam edges throughout the target, therefore the dosimetric accuracy of the plan depends greatly upon the fidelity of the penumbra representation and, as stressed earlier, special care must be taken during treatment planning system commissioning. It is strongly recommended that the measuring of the beam data for the commissioning of an IMRT TPS be carried out in a similar way to a stereotactic treatment planning. A close agreement between measured penumbra and the calculated one has been found with the diamond detector [2.25, 2.29]. A diamond detector seems to be suitable to measure either penumbra and output factors and, if available, could be a good alternative to film dosimetry [2.25, 2.27]. If there is insufficient spatial resolution in the detector used, discrepancies of more than 10% between measured and calculated profile can be found. These discrepancies are emphasised in high dose gradient regions. In Figure 2.9 a comparison between measured and calculated dose profiles is shown. The calculation was performed using the same TPS commissioned using first a 0.4 cm^3 IC and then a diode.

Beside penumbra, further parameters are essential to characterise the MLC manufacture in the optimisation module. Some MLCs have rounded leaf tips and this kind of design must be correctly accounted for by the TPS, since the leakage at abutting leaf ends can be up to 20%. Most of the IMRT TPSs take the effect of the rounded leaf tip into account by assuming a shift

in the position of the field edge depicting the penumbra distribution near the leaf end. For example, in the Varian inverse TPS the leaf transmission offset parameter is called *Dosimetric Leaf Separation* (DLS). Different methods to measure this parameter have been proposed [2.1, 2.13, 2.14]. A more accurate way of taking into consideration the effect of the leaf tip curvature is by modelling it with a transmission function. This will lead to increased accuracy in fluence calculation in the dynamic technique.

Transmission value is a mandatory parameter: in a DMLC plan, the leaf transmission can contribute up to 6% of the total dose depending on the swept field width [2.1, 2.14, 2.15].

Actually, some remarks must be made on the necessity for a direct measurement of all these parameters. It must be emphasised that the delivered dose, especially in DMLC, is influenced in a complicated way by head scatter, transmission through the leaves, geometry and leakage. Most of these parameters attain different values depending on the position of the measurement [2.14] although for each parameter a unique value is allowed by the TPS. The effect of different transmission and DLS values, within a reasonable range, has been tested for the Cadplan TPS (Varian) [2.12]. The results indicate that for values around the mean measured ones this particular TPS is not very sensitive. This gives rise to the idea introduced by Van Esch [2.12] that is, to characterise the TPS with empirical values that produce an optimal correspondence between measurements and calculations. Table 1 carries measured values of dosimetric leaf separation and average transmission factor for some MLC and mMLC commercially available.

Table 1: DLS and transmission values for some MLC and mMLC

	Varian Millennium 120 leaves		Elekta 80 leaves	BrainLAB m3 52 leaves	3DLine mMLC 48 leaves
Energy (MV)	6	18	6	6	6
DLS (mm)	2.0	1.8	—	1.5	—
Average transmission %	1.6	1.7	2.0	2.0	1.0

2.3.2 Commissioning an IMRT treatment planning system

The verification of dosimetric accuracy of an IMRT planning system should follow a systematic sequence. The basic scheme is to proceed from simple to complex tests [2.5, 2.13]. Simple cases should be planned to easily detect the discrepancies between measurement and calculation in case of sub-optimal MLC parameter values and to define the accuracy level in the clinical situation.

As indicated by Ezzel [2.5], the commissioning procedure could be summarised as follows:

- Step 1: preliminary checks, as discussed in a previous section;
- Step 2: tests for a single beam with several specially designed intensity patterns;
- Step 3: tests of multiple beams treating hypothetical clinical targets.

As it would not be practical to validate the system by experimentally checking every possible intensity modulated plan, it is necessary to design a number of tests able to figure out the system limits and faults. In this regard, it is necessary to know how the inverse planning system determines the pattern of beamlet intensities for each field and how it translates the calculated fluence into a delivered one. The way in which the systems handle the interplay between inverse planning and sequencer could affect the accuracy of dose calculation. There are systems which first calculate optimal fluence and subsequently incorporate the effect of parameters such as transmission, penumbra, and leaf-end shape. Otherwise there are systems calculating the final dose based on the actual deliverable fluence.

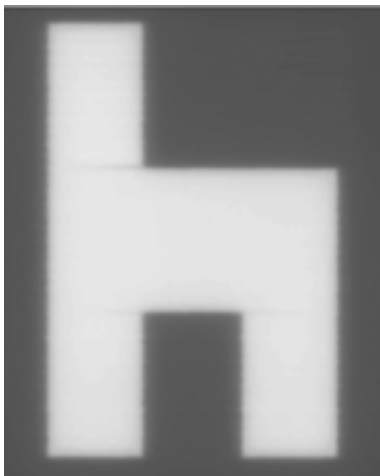


Fig. 2.10 “Chair” test fluence

For the first case, it is possible to plan tests whose aim is to determine if the beam parameter values are accurate. The “chair” test (Figure 2.10) [2.12], for example, was designed to validate the transmission parameter and the effect of rounded leaf edge in a Varian system. In areas with zero fluence the leaf transmission will set a lower limit on the minimum deliverable intensity that can be checked dosimetrically. This kind of test could be used to determine empirically the configuration parameters instead of a direct measurement.

It can be applied to the commissioning of any inverse treatment planning system in which an intensity pattern can be edited independently of the optimisation process.

Going on to step 2, plans should be developed to assess the capability of TPS to produce requested fluence patterns and to verify the accuracy of the dose calculation. Some examples are shown in Figure 2.11 a-d. In a regular geometric phantom, created on a TPS with the same electron density as those used during dosimetry or directly CT scanned, volumes are drawn and single field plans are optimised.

- Plan (a) is designed to produce different dose values to three adjacent target volumes;
- Plan (b) will deliver the same dose to different volumes set at different depths;
- Plan (c) aims to check the limits of the TPS in case of different dose gradients obtained changing dimension and prescribed dose of the treatment volume;
- Plan (d) designed on a sequence of PTVs and OARs, allows a systematic test to evaluate TPS limitations.

Calculated dose distributions will be checked against the measured ones by irradiating a film positioned in a phantom perpendicular to the beam axis, at the depth of the target volume. The comparison between the calculated dose matrix and the measured one at the same depth may be done by means of dedicated software. Relative dosimetry is not sufficient to validate the system, so a careful film dose calibration must be performed. Actually, the accuracy of film dosimetry is strongly related to the processing technique and therefore the simultaneous use of an absolute point dosimeter, like an ionisation chamber, is suggested. Its finite dimension can lead to inaccurate dose measurements due to dose averaging in the active volume [2.22]. The presence of high dose gradient regions, typical of IMRT plans, requires a small volume ionisation chamber, although it is always advisable to perform point measurements in almost homogeneous regions.

Although 2D array detectors are currently available, they cannot entirely replace film dosimetry in IMRT commissioning. In fact, to correctly estimate the accuracy and limits of the IMRT system it is important to use a high spatial resolution dosimeter. The tests proposed can be run periodically to evaluate the long term stability of the whole system. Actually, some TPSs do not allow a single field optimisation, therefore the user is forced to study a multi-field plan even if it is then possible to verify field by field.

To test the IMRT system comprehensively, a series of plans that mimic clinical target and organ at risk (OAR) geometries should be designed. For example, a C shape PTV (Planning Target Volume) surrounding a critical organ can be drawn in a geometric phantom [2.30]. A plan will be optimised setting different constraints on the PTV and OAR to determine their effects on the optimised dose distribution. In this case, film measurements can be performed along different planes. It should be pointed out that coronal planes yield accurate results if careful film calibration is provided while axial film measurement may be less accurate because of the depth dependence of the film [2.32]. The latter measurement strategy together with point ionization chamber measurements could be chosen in clinical cases.

Similar procedures can be used for IMAT: test plans of increasing complexity should be created, designing a series of targets in the geometric phantom. The first step is a dynamic arc plan conforming to a spherical target (it is important to test plans for the smallest spherical target dimensions treated in clinical practice). The next step is to move to a complete IMAT plan with superimposing arcs, conformed to a concave shaped target.

The definition of a level of accuracy or acceptance criteria for an IMRT plan is not a simple issue. Different aspects could influence the dosimetric accuracy: complexity of the plan, high gradient related problems, etc. It is strongly recommended that the accuracy and the limits of the system be evaluated in different situations, similar to clinical ones, and then, as emphasised by Ezzel [2.5], the acceptable level of accuracy must be defined to account for any particular clinical situation. In any case, it is reasonable that in a low gradient high dose area the accuracy achieved would not be higher than 5% for film dosimetry and of the order of 3% for absolute dose measurements with an IC. In high dose gradient regions and low dose value areas, the discrepancy between calculated and measured dose distribution can be up to 10% or more. It is therefore recommended to evaluate such discrepancies for each clinical case. High dose gradient regions are difficult to evaluate for a single field but in a clinical situation, where multiple fields are used, the verification of the whole plan could be less critical. An interesting approach to analyse the agreement between TPS dose matrix and measured dose map is the g function introduced by Low [2.7]. The idea is to summarise the differences in dose values and in *distance to agreement* (DTA) in one parameter. The usefulness of these parameters will be explained in the next chapter.

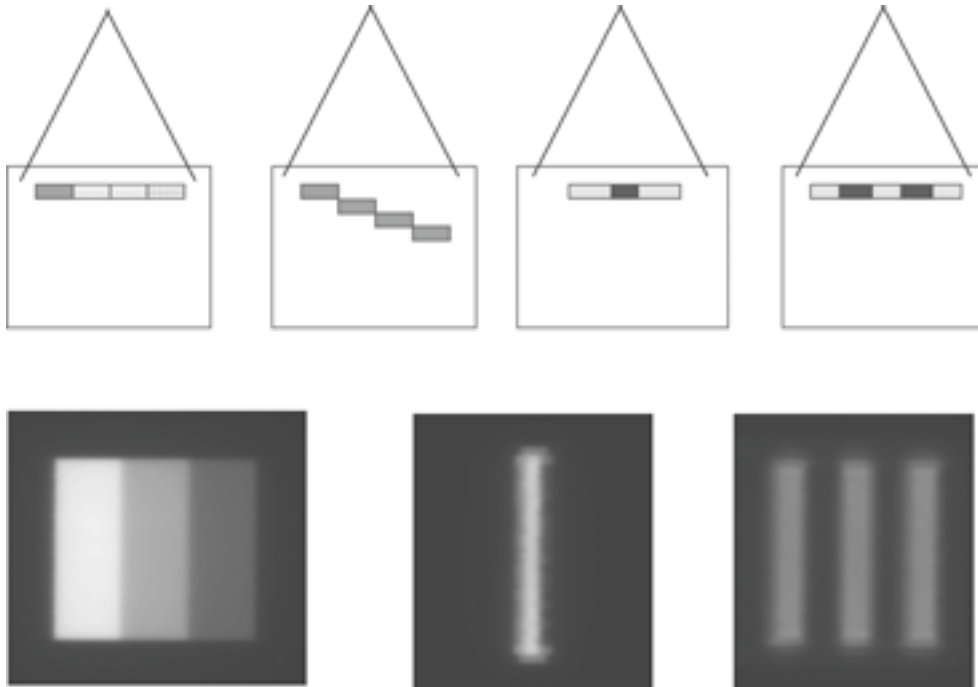


Fig. 2.11 Different volumes at different dose drowned in a mathematical phantom [(a), (b), (c), (d)] and related fluences [f-(a), f-(b), f-(c), f-(d)]

References

- 2.1 T LoSasso, CS Chui and C Ling "Physical and dosimetric aspects of a multileaf collimation system used in the dynamic mode for implementing intensity modulated radiotherapy" *Med. Phys.* 25 (10):1919-1927;1998.
- 2.2 CS Chui, S Spirou and T LoSasso "Testing of dynamic multileaf collimation" *Med. Phys.* 25 (5):635-641;1996.
- 2.3 DA Low, JW Sohn, EE Klein, J Markman, S Mutic, and JF Dempsey, "Characterization of a commercial multileaf collimator used for intensity modulated radiation therapy" *Med. Phys.* 28 (5):752-756;2001.
- 2.4 C Garibaldi, R Azzeroni, F Cattani, R Cambria, G Tosi, R Orecchia, "High leaf speed effects in delivery of intensity modulated radiotherapy with a micro-multileaf collimator" *Radioth. Oncol.* 68 (Suppl 1): S97; 2003.
- 2.5 GA Ezzel, JM Galvin, DA Low, JR Palta, I Rosen, MB Sharpe, P Xia, P Xiao, L Xing, CX Yu "Guidance document on delivery, treatment planning, and clinical implementation of IMRT: Report of the IMRT subcommittee of the AAPM radiation therapy committee" *Med. Phys.* 30(8):2089-2115;2003.
- 2.6 DA Low "Quality Assurance of Intensity-Modulated Radiotherapy" *Seminars in Radiation Oncology.* 12(3):219-228;2002.
- 2.7 DA Low, WB Harms, S Mutic, and JA Purdy "A technique for the quantitative evaluation of dose distributions" *Med. Phys.* 25 : 656-661 ;1998.

- 2.8 CX YU, XA Li, L Ma, D Chen, S Naqvi, D Shepard, M Sarfaraz, TW Holmes, M Suntharalingam, CM Mansfield « Clinical implementation of Intensity-Modulated Arc Therapy” *IJROPB* 53:453-463;2002.
- 2.9 E Wong, JZ Chen, J Greenland « Intensity-Modulated Arc Therapy simplified” *IJROPB* 53:222-235;2002.
- 2.10 CR Ramsey, KM Spencer, R Alhakeem and AL Oliver “Leaf position error during conformal dynamic arc and intensity modulated arc treatments” *Med. Phys.* 28:67-72;2001.
- 2.11 G Grebe, M Pfaender, M Roll, L Luedemann, RE Wurm “Dynamic arc radiosurgery and radiotherapy: commissioning and verification of dose distributions” *IJROPB* 49:1451-1460; 2001.
- 2.12 A Van Esch, DP Huyskens, J Bohsung, P Sorvari, M Tenhunen, M Paiusco, M Iori, P Engstrøm, H Nystrøm “Acceptance tests and QA procedures for the clinical implementation of IMRT using inverse planning and the sliding window technique: experience from five radiotherapy departments” *Radioth. Oncol.* 65(1):53-70;2002.
- 2.13 M Esser, M de Langen, MLP Dirx, BJM Heijmen “Commissioning of a commercial available system for intensity-modulated radiotherapy dose delivery with dynamic multileaf collimation” *Radioth. Oncol.* 60:215-224;2001.
- 2.14 MR Arnfield, JV Siebers, JO Kim, Q Wu, PJ Keall, R Mohan “A method for determining multileaf collimator transmission and scatter for dynamic intensity modulated radiotherapy” *Med. Phys.* 27: 2231-2241;2000.
- 2.15 EE Klein, DA Low, JW Sohn, JA Purdy “Differential dosing of prostate and seminal vesicles using dynamic multileaf collimation” *I.J.R.O.B.P.* 48(5) :1447-1456;2000.
- 2.16 W Duthoy, W De Gerssem, K Vergote, M Coghe, T Beterberg, Y De Deene, C De Wagter, S Van belle, W De Neve “Whole abdomino-pelvic radiotherapy (WAPRT) using intensity-modulated arc therapy (IMAT): first clinical experience” *I.J.R.O.B.P.* 57:1019-1032; 2003.
- 2.17 AL Boyer and Shidomg “Geometrical analysis of light-field position of a multileaf collimator with curved ends” *Med. Phys.* 24:757-762;1997.
- 2.18 AM Stell, JG Li, OA Zeidan and JF Dempsey “An extensive log-file analysis of step and shoot intensity modulated radiation therapy segment errors” *Med.Phys.* 31:1593-1602; 2004.
- 2.19 J Van Dyk, RB Barret, JE Cygler, PC Shragge “Commissioning and quality assurance of treatment planning computers” *IJROPB* 26:261-273;1993.
- 2.20 B Fraass, K Doppke, M Hunt, G Kutcher, G Starkschall, R Stern, J Van Dyke “American Association of Physicists in Medicine Radioation Therapy Committee Task Group 53: quality assurance for clinical radiotherapy treatment planning” *Med.Phys.* 25:1773-1829;1998.
- 2.21 GJ Budgell, JH Mott, PC Williams and KJ Brown “Requirements for leaf position accuracy for dynamic multileaf collimation” *Phys. Med. Biol.* .45:1211-1227;2000.
- 2.22 DA Low, P Parikh, JF Dempsey, S Wahab, S Huq “Ionizatin chamber volume averaging effects in dynamic intensity modulated radiation therapy beams”, *Med.Phys.* 30: 1706-1711;2003.
- 2.23 MB Sharpe, MB Miller, D Yan, JW Wong “Monitor unit settings for intensity modulated beams delivered using a step and shoot” *Med.Phys.* 27:2719-2725;2000.
- 2.24 CW Cheng, IJ Das, MS Huq, “ Lateral loss and dose discrepancies of Multileaf collimator segments in intensity modulated radiation therapy” *Med.Phys.* 30(11):2959-2968;2003.

- 2.25 WU Laub, T Wong, “ The volume effect of detectors in the dosimetry of small fields used in IMRT” *Med.Phys.* 30(3):341-347;2003.
- 2.26 F Haryanto, M Ippel, W Laub, O Dohm, F Nusslin, “ Investigation of photon beam output for conformal radiation therapy-Monte Carlo simulations and measurements” *Phys. Med.Biol.* 47:N133-N143;2002.
- 2.27 M Bucciolini, F Banci Buonamici, S Mazzocchi , De Angelis, C Onori, GAP Cirrone “ Diamond detector versus silicon diode and ion chamber in photon beams at different energy and field size” *Med. Phys.* 30(8):2149-2154;2003.
- 2.28 MM Aspradakis, GD Lambert, A Steele “Elements of commissioning step and shoot IMRT: delivery equipment and planning system issue posed by small segment dimensions and small monitor units” *Med.Dos.* 30 (4):233-242;2005.
- 2.29 F Garcia –Vicente, JM Degado, C Peraza “ Experimental determination of the convolution kernel for the study of the spatial response of a detector” *Med. Phys.* 25:202-207;1998.
- 2.30 J Bohsung, S Gilles, R Arrans, A Bakai, C De Wagter, T Knoos, BJ Mijnheer, M Paiusco, BA Perrin, H Wellereerd, P Williams “ IMRT treatment planning: a comparative inter system and inter-centre planning exercise of the ESTRO QUASIMODO group” *Radioth. Oncol.* 76(3):354-361;2005.
- 2.31 AM Bergman, K Otto, C Duzenli, “ The use of modified single pencil beam dose kernels to improve IMRT dose calculation accuracy” *Med.Phys.* 31(12):3279-3287;2004.
- 2.32 S Gilles, C De Wagter, J Bohsung, B Perrin, P Williams, BJ Mijnheer “ An inter-center quality assurance network for IMRT verification: results of the ESTRO QUASIMODO project.” *Radioth. Oncol.* 76(3):340-353;2005.
- 2.33 JPC van Santvoort and BJ Heijmen, “Dynamic multileaf collimation without “tongue-and-groove” underdosage effects” *Phys. Med. Biol.* 41:2091-2105;1996.
- 2.34 MN Graves, MNA. V. Thompson, MK Martel, DL McShan and BA Frass, “Calibration and quality assurance for rounded leaf-end MLC system”, *Med. Phys.* 28 (11);(2001)
- 2.35 JG Li, JF Dempsey, L Ding, C Liu and J Palta, “Validation of dynamic MLC-controller log files using a two-dimensional diode array” *Med. Phys.* 30 (5):799-805;2003.
- 2.36 DW Litzenberg, JM Moran, and BA Frass, “Verification of dynamic and segmental IMRT delivery by dynamic log file analysis” *J. Appl. Clin. Med. Phys.* 3:63-72;2002.

3. Pre-clinical Dosimetry of IMRT treatments

3.0 Sommario

L'implementazione clinica delle tecniche a Modulazione di Intensità richiede l'applicazione di precisi protocolli di Assicurazione di Qualità pre-trattamento sul singolo paziente, al fine di verificare l'accordo tra la distribuzione di dose calcolata dal sistema di piani di trattamento (TPS) e quella effettivamente erogata. Oltre alle criticità tipiche della tecnica (alti gradienti spaziali interni al campo, prossimità agli organi critici) va considerato il fatto che ciascun trattamento IMRT (Intensity Modulated Radiation Therapy) è "specifico per il singolo paziente", nel senso che la generazione della modulazione avviene tramite combinazioni di segmenti o di velocità delle lamelle a priori differenti per ciascun paziente.

Il presente lavoro si è incentrato in particolare sulle procedure di confronto, sulle tecniche di misura e sulla scelta dei parametri migliori per valutare la qualità dell'accordo tra distribuzione di dose misurata e calcolata. Resta aperto il problema di definire un "cut off", in termini di pazienti trattati, di campi verificati o quant'altro, oltre il quale modificare le procedure rendendole meno onerose; si tratta di un punto estremamente delicato per il quale ciascun centro che impieghi la IMRT nella pratica clinica dovrà identificare una soluzione sulla base della propria esperienza.

Per quanto riguarda le procedure, in pratica nessuno impiega la dosimetria in vivo nella routine clinica della IMRT. L'approccio standard alla verifica dosimetrica dei trattamenti a modulazione di intensità consiste nel trasferire la modulazione su un fantoccio (tramite l'opzione "copy to phantom" o similare del TPS), selezionare punti, linee o piani di interesse, e confrontare la dose prevista sugli stessi con quella misurata. Il fantoccio può essere di differenti forme e composizione [cubico, cilindrico, antropomorfo, in acqua solida o PMMA (polimetilmetacrilato), con eventuali disomogeneità] e la sua scelta dipende anche dalla tecnica di irraggiamento impiegata (fantocci cubici, per esempio, non sono particolarmente indicati per l'impiego in tecniche rotazionali); anche la strategia di verifica dipende dalle preferenze del singolo Centro. Sono possibili opzioni la verifica simultanea di tutti i campi a gantry fissato oppure a gantry effettivo, ovvero la verifica dei vari campi uno per uno, ancora a gantry fissato o effettivo; ciascun metodo presenta vantaggi e svantaggi, discussi con maggior dettaglio nel testo originale.

Per quanto riguarda le tecniche di misura, nel caso in cui si scelga di verificare la dose assoluta in punti selezionati la scelta più conveniente è quella

delle camere di ionizzazione; va tenuto presente che, a causa dei gradienti di dose elevati, possono verificarsi effetti di media sul volume sensibile della camera, e questo impone l'uso di microcamere e la scelta di punti di misura a basso gradiente di dose. La scelta usuale per la verifica di un piano IMRT consiste, usualmente, non nel confronto tra dosi puntuali, ma tra la distribuzione di dose misurata su un piano e quella calcolata dal TPS sul piano corrispondente. La misura della distribuzione di dose su un piano viene di regola effettuata con film-dosimetria; l'argomento è ampiamente discusso nel testo inglese. Le procedure di film dosimetria sono molto complesse e dipendono da numerosi parametri; è un argomento ancora controverso, per esempio, quale sia la miglior tecnica di calibrazione del film e se esista un film in cui il contributo di sovrarisposta alle basse energie sia trascurabile. I film di impiego comune sono i Kodak XV2 ed EDR2; i secondi, caratterizzati da una minore sensibilità, consentono la verifica globale del trattamento senza "rescaling" delle dosi e sembrano avere minore dipendenza dallo spettro della radiazione incidente e dalle condizioni di sviluppo, uno dei punti più critici dell'intera procedura. Va anche tenuto presente che la fase di digitalizzazione del film può introdurre errori se lo scanner impiegato non risponde alle specifiche minime richieste in termini, ad esempio, di uniformità spaziale di risposta ovvero di precisione nella dimensione del pixel.

L'onerosità della film dosimetria rende particolarmente utili le matrici di rivelatori, che consentono, a spese di una inferiore risoluzione spaziale, di ottenere la misura della distribuzione di dose in tempi molto rapidi. La dimensione e la disposizione spaziale dei rivelatori (diodi o camere) all'interno della matrice variano a seconda del modello scelto; nel caso in cui le dimensioni del rivelatore siano significativamente maggiori del "pixel size" nella matrice di dose calcolata, il software associato dovrà necessariamente effettuare una media spaziale prima di procedere al confronto.

Se il rivelatore scelto (film o matrice) è stato calibrato in termini di dose assoluta ed il suo corretto funzionamento in questa condizione è stato accuratamente verificato, le misure 2D consentono di evitare l'impiego della camera di ionizzazione, che è sempre complesso per la necessità di posizionare accuratamente la camera in una regione a basso gradiente di dose. Viceversa, alla misura dell'accordo tra distribuzioni normalizzate dovrebbe sempre venire associata una misura di dose assoluta nel punto di normalizzazione.

Per quanto riguarda infine la scelta dei parametri da impiegare nel confronto tra distribuzione di dose misurata e calcolata, occorre osservare che in linea di principio potrebbero essere utilizzati gli stessi in uso nelle tecniche

convenzionali, ma che questi non sono l'ideale in IMRT. In particolare, le misure di dose puntuale ottenute scegliendo punti corrispondenti sulle due distribuzioni presentano ancora problemi legati al gradiente di dose; anche se non vi sono ovviamente effetti di volume dovuti alla dimensione della camera o errori di posizionamento, le mappe di dose calcolata e misurata devono essere registrate spazialmente prima del confronto, e anche un piccolo errore sulla registrazione può portare a scarti non trascurabili. Un problema analogo nasce con i profili di dose; in più, mentre nella terapia standard la singola coppia di profili ortogonali è abbastanza rappresentativa dell'accordo anche sui profili non misurati, in IMRT questo non è assolutamente vero. Nel caso delle curve di isodose, infine, è evidente che possono dare una ottima indicazione nelle regioni ad alto gradiente spaziale, ma sono scarsamente significative in regioni a basso gradiente nelle quali a scarti in dose trascurabili possono corrispondere anche notevoli differenze nelle curve.

Per adattare i parametri usuali alla IMRT è stato introdotto il concetto di "matrice", che unisce i concetti di accordo in dose (valido nelle regioni a basso gradiente di dose) e "Distance to Agreement" (DTA, valido nelle regioni ad alto gradiente di dose) in un parametro unico. Rimandando al testo completo per la trattazione di questo parametro, che è piuttosto complessa, è comunque necessario sottolineare che la valutazione globale dell'accordo tra distribuzione di dose calcolata e misurata, soprattutto nella fase iniziale di impiego clinico, quando ancora l'esperienza acquisita non è esaustiva, non dovrebbe prescindere dall'impiego combinato di tutte le fonti di informazione disponibili.

Restano al di fuori di questo lavoro i problemi di posizionamento del paziente, volutamente rimandati a trattazione in sede più adatta. Per le indicazioni bibliografiche si rimanda alla bibliografia di approfondimento di questo capitolo.

3.1 Introduction

Intensity Modulated Radiation Therapy requires a dedicated QA (Quality Assurance) procedure for each patient to be treated. The aim of patient QA is to check the agreement between the dose distribution calculated by the TPS and the effective one. The main reason for which patient QA is recommended is that the sharp dose gradients found in IMRT, make the deviations between calculated and real dose distribution critical even if they are very small, especially in regions close to organs at risk. In addition, each IMRT plan is strictly specific to the patient because the various segment shapes and

Monitor Units (in step and shoot mode) or leaf position and leaf speed (in dynamic mode) may be quite different, even if the shape of the target and organs at risk are very similar, because it is dependant on multiple factors, each of them influencing the way in which a certain dose is effectively released to the patient.

It is still an open question whether there should be a cut-off value (in terms of number of fields planned and verified, for example) that makes single patient QA an unnecessary time-consuming procedure. The question is controversial and no definitive answer may yet be given; each centre has to investigate the question and to take a decision based on its own experience.

In this chapter the following topics will be discussed:

- general procedures for patient QA
- methods of dose measurement for IMRT treatment plan verification;
- procedures for dose comparison between TPS and measurements;
- parameters to be evaluated.

3.2 Procedures

The first step in the patient QA procedure is always the production of a calculated dose matrix to be compared to the measured one. Because of the well-known technical difficulties of “in-vivo” dosimetry, the patient treatment verification is done using a solid water or PMMA (PolyMethylMethAcrylate) phantom, in a well defined geometry. The phantom can be scanned and the CT images saved into the TPS (Treatment Planning System). As an alternative, a phantom with the same dimension and electron densities as the real one may be created by TPS routines.

The TPS should offer the possibility of importing IMRT fields from a patient plan into the phantom. This option is usually known as “QA plan” or “copy to phantom”. The dose distribution in any plane of the phantom can subsequently be calculated and exported, allowing comparison with the measured data in data processing software. The dose calculated in the plane of measurement is extracted from the TPS either through point doses, line profiles or two dimensional dose matrices and may be compared to the measured data by means of point dose measurements (ionisation chambers, TLDS, diodes and diamond detectors), one and two dimensional detector array measurements or film irradiation.

In particular, two strategies are in common use: treatment plan verification either of each IMRT field test plan (case 1) or of the complete treatment plan

(case 2). For both these types of verification, the use of bidimensional detectors is recommended, in particular films or detector arrays; details about detectors will be given later in this chapter. In case 1, the geometry of irradiation is orthogonal: the detector plane is perpendicular to the axis of the beam and the comparison between measured and calculated dose makes it possible to identify deviations on all the surfaces of every field, but does not take into account the eventual effects of compensation due to the contribution of the other fields. In this case, the detector is usually in a coronal plane, over the couch, and gantry angle is 0° .

In case 2, cylindrical phantoms are usually employed, with the axis parallel to gantry rotation; the detector (film in this case) is normal to the phantom main axis, simulating in some way an axial cut of an ideal patient. In this way it is possible to irradiate all the fields and to integrate them; however, eventual compensations can mask discrepancies in single fields. It is also possible to irradiate the detector in a planar geometry, (as in case 1), with all the fields at the same time; also in this case compensation effects may influence the results.

The first method is very easy to realize and it measures effectively the entire matrix of modulation for every field; the only real limitation is the fact that the influence of gravity is not taken into account. Moreover, it may be used with detector arrays and not only with films. The second method is faster, the geometric representation is more similar to the clinical case and the results include mechanisms for compensating errors; however compensation effects may differ from the real case and at worse they may underestimate the real deviation.

There are several commercial phantoms that can be used for this verification. They can be of different shapes (parallelepiped with slabs, cylindrical, anthropomorphic) and materials (Dry Water, plastic) but for routine controls we suggest the use of a slab phantom in which the film is positioned in a coronal orientation. This setup is easier to perform and is more reproducible (also for TPS simulation) than the one with the film in the sagittal position. Moreover, in the sagittal position the air gap between two slabs can cause dose errors. Consequently, the first method described above is preferable, however each centre must choose the method that best fits its needs. It should be noted that this method is not the best choice for techniques like conformal arcs or IMAT.

The steps of the whole procedure can be summarized as follows. Obviously some steps depend on the chosen detector (film or array):

- import each IMRT field or complete treatment plan from the patient plan into a phantom designed for TPS routine;
- deliver the complete plan or individual beam to film or detector array;
 - only if films are used:
 - film calibration by exposing one or more films (see below) to given doses;
 - developing all films (together with a non-irradiated film for the fog) at the same time;
 - reading of the films with a densitometer or film scanner, performed at the same time.
 - in every case:
 - analysis of the results with a dedicated software: the comparison is made with the dose matrix calculated and exported by the TPS.

Unlike the step and shoot technique, for which the monitor units (MUs) can be scaled, for the sliding window technique, the normalization of the single field test plan is such that MU are identical to those of the corresponding field in the original patient plan because the dose delivery depends on the speed of each leaf. If individual beam delivery is to be performed, the dose contribution of a single beam is low (usually less than 50 cGy) and one can choose XV-Omat film that is more sensitive than EDR2 film. As discussed in the following sections, however, the XV-Omat film has some dependence on beam energy and the use of this film for field sizes more than 10 cmx10 cm and at large depths must be carefully evaluated [3.19]. The use of a filter that removes low energy scattered photons can be useful to reduce the error in film response and allows the use of a single calibration curve [3.8, 3.18].

When a complete plan is delivered, the choice of EDR2 film is more suitable because its specific characteristics (large dynamic range, less energy dependence: see next sections). With this film it is not necessary to scale the MU and the same dose per fraction used for the patient plan can be given to the film. This avoids the problem of segments with very low MU after the dose scaling (in step and shoot mode) and the problem of forcing the MLC leaves to move faster (in dynamic mode) [3.14]. Obviously, the rescaling problem does not apply in the case of arrays of detectors, that usually show a linear behavior over a large range of doses.

Additionally, absolute dosimetry may be performed using an ionization chamber; this is mandatory if two dimensional dosimetry is not absolute.

The use of ionization chambers in IMRT dose verification requires a very careful procedure. As stated in the literature [3.31; 3.32], the use of standard ionization chambers (e.g Farmer type chambers, 0.6 cc) for absolute dosimetry may lead to wrong results, due to volume effects, unless the dose gradient around the chamber position is negligible in relation to the dimension of the chamber. Another important point is the risk of partial chamber volume coverage in some segments; in fact if the chamber section is larger than the minimum segment size, the segment border may pass through the chamber volume for some segments.

In view of the above consideration, it is mandatory to use a small volume chamber unless a carefully chosen point is used. Different small size chambers are now available; sensitive volumes may be as small as 0.007 cubic centimeters (i.e. about 100 times smaller than a standard Farmer type chamber). Using these small volume chambers, however, requires some additional consideration. Due to small sensitive volume, the leakage current may be very significant; reference [3.31] shows that disregarding leakage may lead to dose underestimates of up to 16% when using a 0.009 cc volume ion chamber. This result depends not only on the chamber type but also on the electrometer. Indeed, it is necessary to check the influence of leakage current for each electrometer – chamber combination.

Another important effect of leakage current is the underestimation of the dose contribution coming from segments in which the chamber is fully covered by leaves. In this case, the signal may be lower than the leakage current, so leading to an underestimation of the global dose. In reference [3.33], which deals with the behavior of a commercial diode matrix, dose response between diodes and a PinPoint chamber has been investigated. The authors report ion chamber dose underestimations ranging up to 3.2% with respect to diodes, and this discrepancy is attributed to the latter effect.

Finally, great care must be taken in assessing the polarity response of small volume chambers; values as large as 1.8% are reported for Exradin A14SI chamber [3.32].

Given the above consideration, a reasonable level of action for investigating discrepancies between ion chamber measurements and treatment plan may be 3 – 4% in high dose – low gradient regions [3.32]. If the chamber is not well positioned however (for instance if the chamber lies in a high dose gradient region), larger errors may occur, particularly when using small volume chambers. In IMRT treatments, in fact, dose gradients as large as penumbra regions gradients may occur, so leading to large errors in these

regions even for small (i.e. 1÷2 mm) chamber positioning errors.

A crucial point in IMRT delivery is patient positioning and immobilization and the relative checks. This topic is beyond the arguments of this chapter.

3.3 Film dosimetry

Film dosimetry is a well established method to verify dose distributions in phantoms or to perform quality control tests of radiation beams. In particular, it is the main method used by every centre implementing the IMRT technique for its excellent characteristics.

In this paragraph, the characteristics of films will be illustrated, and the critical points of this dosimeter will be discussed.

The main characteristics making the film suitable for radiation dosimetry are:

- high spatial resolution, limited only by the systems for film reading;
- integrating dosimeter
- easy to handle

On the other hand, the main problem when using radiographic film is represented by the existence of several parameters which influence the film sensitivity:

- photon beam energy;
- film plane orientation with respect beam direction;
- emulsion differences among films of different batches, films of the same batch or even in the same film;
- processing conditions;
- type of densitometer or film reader.

The photon beam energy dependence is the most troublesome and unavoidable variable: in fact, for a given photon beam quality, the photon energy spectrum changes with both depth and field size due to the variation in phantom scatter and beam hardening.

The results of film plane orientation and depth-field size dependence are reported in a paper of Danciu for two types of films [3.1]: from this study it can be concluded that good dosimetric results can be obtained irradiating film of the same batch, from small field sizes (5 cmx5 cm) up to 15 cmx15 cm, at moderate depths (up to about 15 cm), using a single calibration curve for a 10 cm x 10 cm field during perpendicular exposure [3.1, 3.2, 3.3, 3.4, 3.5, 3.6].

The results shown so far were obtained for fields not smaller than 5 cm x 5 cm. Different studies [3.5, 3.6] reported an overestimation of the film compared to ionization chamber of 10% in depth dose data for field sizes less than 10 cm square and depths of about 12 cm.

In IMRT technique, the radiation field is composed of multiple fields and their outside-penumbra regions, where the film is known to show large over-response [3.4, 3.7]. The response of film for the composite field in IMRT has been evaluated against ion chamber measurements [3.8]: the over-response in the outside penumbra regions of the smaller segments (or beamlets) are suppressed by the relatively large signal of the infield profiles corresponding to the greater field sizes. The outside penumbra region of the composite field consists of those of the beamlets profiles, and therefore shows a relatively high over-response. It was also found that this over-response depends on the depth in phantom (the max deviation is 8 % at 10 cm depth in the low-dose region), and that it can be reduced, by using lead filters, to a few percents. The selection of the thickness of the filter and the optimal film-filter setting must be determined experimentally by each Centre because it depends on the energy of the photon beam, the depth in phantom and, the orientation of filters against the beam incident direction (film parallel or perpendicular to the beam). In the above reported study, e.g, the use of filters in the perpendicular setup caused an under-response of 8 %, as a maximum, in the infield regions of an inverse-pyramid modulated beam.

It is well known the effect of film processing on the OD: the difference in chemical composition of the processing liquids, the temperature, and the processing time will affect the shape of the sensitometric curve [3.10]. Bos et al. found that the differences in film processing have a larger effect on the shape of the sensitometric curve than a difference in batch composition. The effect of film processing can result in a higher OD for the same dose and this enhanced sensitivity reduces the dynamic range of films because saturation occurs at lower dose values.

The effect of film scanner on the shape of the sensitometric curve has been analyzed on five scanners (Wellhöfer WD102, Multidata 9721, Konica KFDR-S, X-Rite Model 301, Vidar VXR-12) [3.2]. The shape of the curve depends obviously on the type of film. It was found that for Kodak X-Omat V film the shape is similar for all densitometers and there is a small variation (from 2.7 to 3.0 OD) only for high doses (150 cGy). There is a larger variation in absolute values of OD for CEA film in the saturation area of the film scanner (at 100 cGy, OD varies from about 2.6 to 3.4).

The role of CCD film digitizers in film dosimetry has been widely analyzed in the paper of Mersseman et al. [3.11]. For a CCD scanner at 12 bit, the main characteristics can be summarized as follows:

- warm-up effect of fluorescent lamp (that cause a drift in the first 20 min after switching on the digitizer);
- the noise is very high for Optical Density above 2 which corresponds approximately to a dose of 80-90 cGy for a XV film. This can be a limiting problem in IMRT verification where dose per fraction is higher (180-250 cGy) and, if rescaling of doses is necessary, there is the problem of rounded MUs for MLC segment or leaf speed rescaling; the problem is solved with EDR2 films;
- the noise is also a function of the digitizing speed and resolution: for a given resolution, the lower the speed the lower is the noise. But, when lowering the speed, the discrepancy between actual OD and measured OD increases; the greater the resolution, the greater is the noise; a resolution of 75 dpi (dots per inches) with a speed of 20 ms/line gives the optimal SNR;
- the internal light scatter is a potential source of error near optical discontinuities: a collimation of the area of interest and a shielding of the most transparent areas on the film minimized this effect;
- the use of conversion table that transforms the signal measured by the CCD into OD and then the use of a second conversion of OD into Dose introduces inaccuracy and reduces the information contained in the film: a direct conversion from measured signal and dose seems to be more accurate.

The problem of noise can be partially solved with a more expensive 16-bit CCD film digitizer, but more extensive studies should be carried with this system. One of the institutions involved in the drawing up of this paper has employed a detailed evaluations of the performances of the VIDAR VXR16-DP scanner, a 16-bit CCD scanner commercially available, showing its excellent characteristics in dosimetry applications [3.24].

There are also commercial film digitizers that are based on a scanning He-Ne laser beam [3.12]. They have less noise compared to CCD scanners, and they have also good performances up to 3.5 OD. On the other hand, they have problem of cross-talk and they must be frequently re-calibrated by the company. Laser scanners undergo the vignetting effect (the laser light will be more attenuated at outer regions due to its increase in pathlength). This effect is taken into account by calibrating the system, but for films with different

tint the attenuation of the laser light can be different and a single calibration would not be sufficient [3.13].

For IMRT verification, the ideal film should satisfy the following characteristics:

- measuring absolute dose with an accuracy of less than 2%;
- being independent from beam energy;
- being sensitive to doses between 5 and 250 cGy;
- being linear in this dose range;
- being insensitive to film processing.

During the recent years several groups have reported the characteristics of a new type of film that seems to satisfy these requirements [3.14, 3.15, 3.16, 3.17]. The Kodak EDR2 ready-pack film has an enhanced dynamic range and a lower sensitivity compared to the XV-Omat film. This is due to the different composition of the emulsion that contains less AgBr grains (1/10 compared with XV-Omat), it has smaller grain size and less silver content. The results are an extended dose range of the characteristic curve and a lower energy dependence. The dependence on the setup geometry is very low for EDR2 films (the percentage depth doses were within 1% for a wide range of field sizes and depths even though the calibration data-set was obtained with film exposed perpendicularly to the beam). EDR2 films were used also for testing IMRT plans by comparison with both a dose matrix of a Treatment Planning System (TPS) and an XV-Omat film. The EDR2 film agreed significantly better with the treatment planning computer than XV-Omat film. However, a recent paper by Yeo *et al* [3.30] suggests the use of a lead filter to avoid dose overestimation when using both type of films.

The low sensitivity of EDR2 film represents an advantage at high doses, but it could be a disadvantage at very low doses, that are important because they can be close to critical organs: in the reported study [3.14], it was found that EDR2 solved depth doses better than XV-Omat even for very low doses. The use of a 16-bit scanner can increase the ability to solve the very low optical densities.

The indicated characteristics of EDR2 film make it very suitable for QC on IMRT since due to its higher saturation dose, it can be used without monitor unit reduction, and therefore providing for a measurement done under exactly the same conditions as for actual patient treatment. This avoids uncertainties introduced by forcing the MLC leaves to move faster (for dynamic treatments) during QA than for patient treatments, rounding off non-

integral MU, and using very low MUs per segment, where some accelerators may have problems in reaching a fully stabilized dose output and uniformity.

The calibration of the film is time-consuming but it has been suggested to perform it during every session in order to minimize the errors due to film storage, exposure conditions, film developer, and scanner variations (whose contribution to the error in film dosimetry has been evaluated to be around 8%).

The use of an accurate calibrated film curve makes possible to use film dosimetry as an absolute dose measurement method. Due to the very low limits usually accepted in the comparison between IMRT calculations and measurements, before using films like an absolute dosimeter an extensive set of test should be planned and executed; as appears from the previous discussion, very different results are obtained from different institutions and each centre should gain a deep experience in film dosimetry before relying only over films for absolute dose measurements [3.1, 3.18].

3.4 Detector arrays

The problems shown in the previous paragraph, make film dosimetry a very time consuming procedure; for this reason detector arrays are gaining an increasing popularity in the IMRT community. A detector array is simply a planar array of detectors embedded in a suitable set-up; the number, type and size of the detectors may vary according to the model. Because a chapter of this paper is dedicated comparing the arrays presently available, no further details will be given here. However, some clinical considerations must be made.

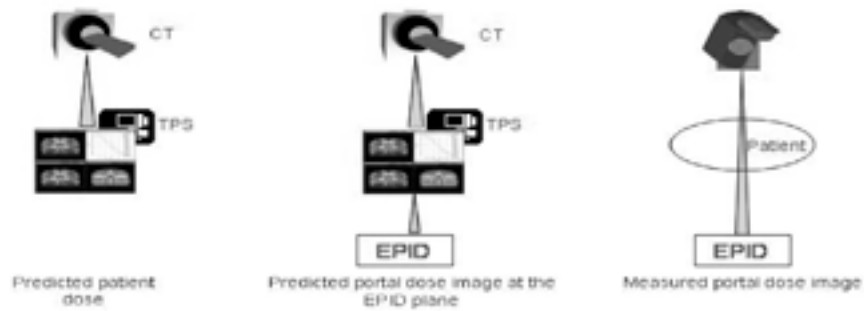
- An array of detectors can not substitute film dosimetry in the commissioning of IMRT, but is a valid substitute for it in routine QA. The main problems of arrays, in comparison with films, are the lower spatial resolution and the fact that they can be used only in a coronal plane, not in a sagittal one; this makes them unsuitable for arc techniques. Although the lower resolution is not a crucial problem (the sample points are chosen so as to be a good representation of the actual dose matrix), they might be placed, for example, along a leaf border, therefore making the result particularly sensitive to effects like “tongue and groove”. On the other hand, the time required for data acquisition and analysis is substantially shorter than for films, therefore reducing both Linac and physicist workload.

- The sharp dose gradient makes the detector size a crucial point. If detector size is large in respect to the dose gradient, some software correction must be employed before comparing measured and calculated dose distributions.
- If the array is used as an absolute dosimeter, dosimetric characteristics of the detectors in terms of field size, depth and dose rate independence, like its short and long term stability, must be carefully checked (see, for example [3.25]). If the array meets all the required specifications, using it as an absolute dosimeter has the great advantage that is fast and does not require the careful positioning that is necessary with a chamber in a low-gradient point. This saves time and the need to repeat the measurement if there are disagreements (if so, if an ion chamber has been used, the problem is raised of whether the disagreement comes from a positioning error or from an effective difference between calculated and measured data).
- In order to determine the usefulness of an array, it is important to take into consideration not only the detectors, but also the quality of the associated software. Poor quality software can make a very good detector array unsuitable for clinical implementation!

3.5 EPID dosimetry

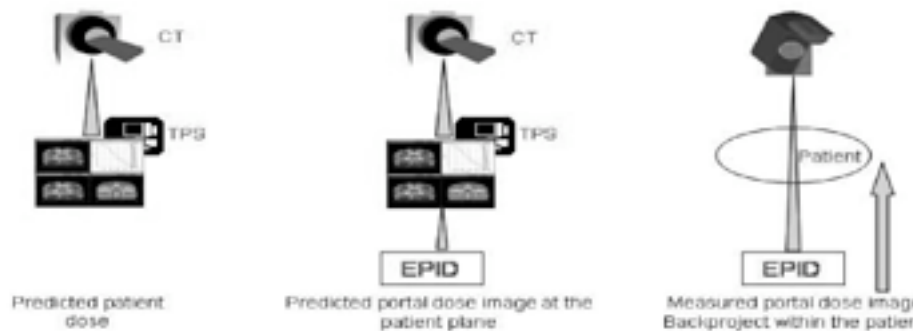
Electronic Portal Imaging Devices (EPIDs) have replaced conventional radiographic films for the acquisition of portal images in radiotherapy and they are very promising for the dosimetric approach. Electronic Portal Imaging Devices produce images that are digital at the origin, immediately available for analysis, and show a good stability of response. Ever since their introduction, their potential for quality control applications has been recognized but their use is limited to institutions which can invest time and effort into developing home-made software required for this kind of application. Up to now EPID systems are still mainly used for verifying patient positioning during conformal, stereotactic or intensity modulated radiotherapy and their use is going to be extended for in vivo dosimetry purposes. The applications of portal dosimetry can be found in the literature for all types of EPID [3.34 ÷ 3-42]. The physical structure of the last generation amorphous silicon based EPIDs is complex and consists of multiple layers of different materials above and below the detector layer of the devices. These systems can acquire large area images of good quality, are highly resistant to radiation damage and present an intrinsic linear dose-response relationship which make these devices suitable for dosimetric application.

Forward approach



Portal dose image is compared to a predicted portal dose image

Backward approach



Comparison of the predicted with the delivered dose distribution in the patient or phantom

There are two approaches to portal dosimetry, both suitable for pretreatment verification and in vivo dosimetry (see next figure). The first one, called “forward approach”, calculates the dose at the plane of the EPID behind the patient and compares it with the EPID measured transmission dose. In this case it is necessary to predict the dose at the EPID level, if this option is not present in the commercial treatment planning system it is necessary to develop a software to calculate the portal dose image [3.42, 3.43]. The second approach, “backward approach” starts from the portal dose image and predicts the dose in a plane within the patient or within a phantom. In this case an algorithm has to be used to back-project the portal dose information in a

plane within the phantom or to reconstruct the dose in the patient by back-projecting the fluence measured with the EPID [3.44 ÷ 3.46]. The latest approach is appealing since it is often more interesting to know and verify the dose in the target volume than at the EPID plane. Moreover 3D dose reconstruction is potentially possible with this method. Portal images can be transformed into ‘dose images’ which have to be correlated with dose value so a relationship between pixel intensity and absolute dose can be established. Due to its complex structure, EPID calibration is more difficult than a simple cross-calibration of pixel response with dose measurements made with an ion chamber in a homogeneous water phantom. This results in dose deposition properties which can radically differ from a homogeneous phantom. Additionally, the presence of high Z materials determines an over-response to low-energy scattered radiation. This problem is of particular relevance in IMRT applications, because it results in a field size dependence which must be taken into account. In order to obtain dose distributions from EPID images, it is necessary to calibrate the device. The approaches found in literature are various but can be split into two groups. In the first one the procedure followed is empirical, for example it can be based on the measurement of field-size-dependent, equivalent EPID phantom-scatter factors. These factors are used to derive a field-size-dependent relationship between EPID pixel values and the ion chamber measurements in a phantom at the center of an open beam [3.47]. The second calibration approach is a mathematical one, based on the convolution method and scatter kernels [3.48 – 3.50].

3.6 Parameters to be compared

Intensity modulation verification requires a substantially new approach to quality assurance from that used for standard therapy. In fact, the sharp dose gradient found not only outside the field edge (as in conformal therapy) but also inside of the field edge, makes the usual parameters of comparison (isodoses, profiles, point measurements) insufficient to completely characterize the agreement between calculated and measured dose distributions. In this paragraph the different parameters available will be discussed with particular attention to the so-called γ -index.

The typical procedure for comparing two dose distributions consists in identifying a “primary” or “reference” dose distribution (usually measured), “a secondary” distribution (usually calculated), registering the two images and in comparing the registered images. Two approaches may be used for image registration: the “classical” one consists of aligning the positions of at least 4 points on the film and on the calculated dose matrix. The points on the

film are obtained by punching the film with a needle in given positions, while for the calculated matrix the coordinates are constructed with a template of fixed points put into the software. This approach may be inaccurate if the images of the punched points appear like a large circle (due to the light passing through the hole) or if the film has moved inside its envelop after being punched. A second approach uses a “centroid” method in which a series of corresponding points are identified in both images to produce the rigid image transformation (that is, a combination of rotation, shift and pixel rescaling, with no distortion) that best correlates the two sets of points. In this case, it may be difficult to identify enough corresponding points with precision; clearly using more point pairs reduces the error. Apart from the chosen protocol, it is mandatory that the origin and axis of the registered coordinate system coincides respectively with the isocenter and the main beam axis, so that every point in the registered space corresponds with couch movements in case of independent dose verification with ion chamber or linear array.

Obviously, no registration is necessary in the case of detector arrays because the coordinates of each detector are directly related to the isocenter.

Once the images have been registered, the agreement between calculated and measured dose distributions must be analysed. Apart from point measurements, in which a single point is chosen on both images and (if necessary) measured with an ion chamber, a qualitative check of the agreement is usually performed by dose profiles along selected lines or isodose comparisons. However, isodoses may show large discrepancies in low dose gradient regions while profile comparisons may show large discrepancies when dose gradients exist in the direction normal to the profiles themselves. Moreover, while in standard fields few profiles may be adequate to check the whole dose map, this is not so for IMRT.

If quantitative comparisons are required, the concepts of “dose agreement” or DA% and “distance to agreement” or DTA [3.26] are employed. These parameters are defined as follow:

- In a low dose gradient region, DA% is defined as the percentage difference between calculated and measured dose;
- In a high dose gradient region, DTA is defined as the minimum distance, in the plane, between a point in the reference dose distribution and the nearest point in the secondary dose distribution that has the same dose.

The DTA and the DA% are quantitative tools but they still have important limitations when applied to IMRT dose distributions. Clearly their applicability is limited to the regions where they are defined. In fact, they have been

introduced for dealing respectively with full dose regions and penumbra regions, that is, in cases where the difference between low and high gradient is unambiguous. Therefore in intermediate gradient regions, like those found in Intensity Modulation inside the field edges, neither of them is fully representative. Some film dosimetry software packages (e.g. RIT113) produce more data sets, each one dealing with a certain dose region gradient; the result is a huge amount of data in which it is very easy not to recognize the significant ones.

To overcome all these problems, a new parameter has been introduced in a paper by Low et al. [3.27]. This parameter, known as γ -index, has gained large diffusion in the IMRT physicist community because it includes in a single data set DA% and DTA. Other papers have discussed the limitations and applications of this parameter to IMRT dose verification [3.28, 3.29] and film dosimetry software developers are introducing the γ calculation inside their codes.

The γ -index is defined as follows. Given a point in the reference distribution, \mathbf{r}_r , and the relative dose D_r , an “acceptance ellipsoid” for point \mathbf{r}_r is defined by :

$$\sqrt{\frac{\delta r^2}{\Delta d_M^2} + \frac{\delta D^2}{\Delta D_M^2}} = 1$$

where $\delta r = |\mathbf{r}_r - \mathbf{r}_c|$ is the distance between the point \mathbf{r}_r and a point \mathbf{r}_c chosen in the secondary distribution, $\delta D = D_r(\mathbf{r}_r) - D_c(\mathbf{r}_c)$ is the corresponding dose difference, Δd_M and ΔD_M the acceptance criteria for distance and dose. The two dose distributions satisfy the imposed constraints in the point \mathbf{r}_r if there exists in the secondary distribution at least one point \mathbf{r}_c for which :

$$\Gamma_r(\mathbf{r}_c, D_c) \equiv \sqrt{\frac{\delta r^2}{\Delta d_M^2} + \frac{\delta D^2}{\Delta D_M^2}} \leq 1$$

This function is called “ Γ function”. We defined “ γ -index” of the point \mathbf{r}_r the minimum value of Γ over the \mathbf{r}_c space, i.e. :

$$\gamma(\mathbf{r}_r) = \min_{\forall \mathbf{r}_c} \left[\sqrt{\frac{\delta r(\mathbf{r}_r, \mathbf{r}_c)^2}{\Delta d_M^2} + \frac{\delta D(\mathbf{r}_r, \mathbf{r}_c)^2}{\Delta D_M^2}} \right]$$

In practice there are two different approaches to γ -index calculation. In the simplest case the calculation is binary: the result of the test is accepted IF $|D(\hat{r}_r) - D(\hat{r}_c)| \leq \Delta D_M$ OR IF inside the circle of radius ΔD_M and center \mathbf{r} , there

exists AT LEAST ONE point \mathbf{r}_c where $D(\mathbf{r}_r) - D(\mathbf{r}_c) \leq 0$ AND ONE where $D(\mathbf{r}_r) - D(\mathbf{r}_c) \geq 0$. Using this simple approach one greatly shortens the calculation time but loses any quantitative information about the intermediate results. The “full” approach, based on the above definition of γ , is more time consuming but preserves all the available information about the agreement between the two dose distributions; in this case the γ values may be statistically analyzed or plotted like histograms.

Some very important characteristics of γ -index must be underlined. It is clear that γ is a point function, i.e. is available also for a sparse set of primary data or (case limit) for a single point measurement like ion chamber. On the contrary, the secondary dose distribution should have a very high resolution for minimizing quantisation errors; as a general rule, the pixel size of the secondary distribution should be less then [3.29] of the limiting distance. This may require resizing of the secondary dose distribution; it is advisable to check the resizing algorithm for the absence of artefacts.

As a general rule, acceptance criteria of 3 % dose difference and 3 mm distance to agreement are adopted. However, the meaning of 3 % has to be carefully understood. Some commercial software normalizes the two dose distributions to a common point and applies the 3 % limit to the normalization dose (i.e., the dose in that point), so obtaining a fixed dose limit value.

This is a possible option but has some implications that should be clear.

- If the agreement between calculated and measured dose is evaluated using renormalized dose distributions, then γ is correct only if the two dose values in the normalisation point perfectly agree. Otherwise, the γ value statistics (e.g., % of points satisfying the condition $\gamma \leq 1$ or other) is not fully significant, because there exists no method to correct the calculated values to take into account the difference between the above two dose values.
- Using a fixed value as dose limit means that the requirement effectively applied depends on the point. In particular, it is greater or lower than 3% if the dose in that point is respectively lower or greater than the normalization dose (e.g.: normalization dose 100 cGy, dose limit 3 cGy means that the effective dose limit is 6 % if point dose is 50 cGy or 1.5% if it is 200 cGy). This implies that the requirement is not applicable to the total dose distribution delivered to the patient, which is obtained by summing the different field contributions.

To overcome these problems, a possible option is to apply the percentage limit to the absolute dose value in every single point. This makes the per-

centage dose limit independent of the point; moreover, because of the linearity of summing doses, the same percentage dose limit applies to each point of the total dose distribution. However, because at low doses this approach becomes very restrictive, it is necessary to define a threshold level and a fixed dose limit, carefully chosen, to be applied under the dose threshold. A reasonable limit for this threshold depends on the accuracy of the low dose measurements; values as low as 10 cGy may be chosen, but this involves very restrictive constraints, so (for example) a reasonable value may be 30% of the maximum dose.

Although γ -index is very useful and widely adopted, it is advisable not to rely on it alone for patient QA. At least a significant sample of point doses, profiles and isodoses should be investigated in every case to best understand the real agreement between measured and calculated dose distributions.

The last point to be discussed is what happens if the measured values are normalized rather than absolute doses (relative film dosimetry, for example). In this case an independent dose verification with an ion chamber is mandatory at a point in a low gradient region. This approach is in fact widely diffused, because the γ values alone (or any other parameter related to the comparison of the two normalized dose distributions) are no longer sufficient for characterizing the agreement between measured and calculated data-

Appendix : Real-time 2D verification tools for IMRT

a.0 Sommario

Il metodo più utilizzato per la verifica di campi IMRT (Intensity Modulated Radiation Therapy) è il confronto tra le distribuzioni di dose ottenute con le pellicole radiografiche in un fantoccio omogeneo con la distribuzione di dose calcolata dal piano di trattamento (TPS-Treatment Planning System). Sistemi 2D a scintillatori per il controllo della fluenza e dispositivi elettronici per l'acquisizione di immagini portali digitali (EPID-Electronic Portal Imaging Device) sono molto diffusi e vantano un'alta risoluzione spaziale. Sul mercato esistono inoltre strumenti 2D per la verifica immediata della dose costituiti da matrici di camere a ionizzazione o di diodi di silicio la cui risposta è facilmente e rapidamente confrontabile con i valori attesi del TPS. L'obiettivo del seguente lavoro è stato confrontare tra loro tre sistemi 2D di verifica in tempo reale: due sono attualmente in commercio, il terzo è un prototipo che è stato sviluppato presso l'Università e l'Istituto Nazionale di Fisica Nucleare di Torino e che è ora in commercio. Le misure si sono

svolte in 9 differenti ospedali italiani; il fine era testare le risposte dei rivelatori al variare dell'acceleratore, del collimatore multilamellare (MLC-Multi Leaf Collimator) e del TPS.

a.1 Introduction

One of the most widely used methods for IMRT verification is to compare the dose distribution calculated by Treatment Planning Systems (TPS) in a simple-geometry phantom with the measured dose distribution with films. If films are normalized to additional ionisation chamber measurements, the dose distribution can be expressed in absolute value. A check of the modulated beam fluence pattern has also been carried out using a 2D-beam imaging system. These methods have their strength in the very good spatial resolution and, when films are properly calibrated, in the good precision obtained for the dose measurement. On the other hand they can be extremely cumbersome and time consuming. The use of EPIDs is also investigated by many authors.

Since some time, tools that allow a 2D verification with matrices of ionisation chambers or silicon diodes are available on the market. In this case, the response is immediately available in a digital form and can be compared to the TPS predictions. The spatial resolution and number of sampling points are inferior to those obtained with films.

The goal of the present tests was to compare the behaviour of two commercial devices and one detector, a prototype that has been developed at the University and INFN of Torino (now commercially available as well). The three detectors have been tested in several hospitals, to be able to measure their performances when different combinations of delivery techniques, multileaf collimators and TPS are used.

a.2 2D verification systems

a.2.1 PTW 2D-Array

The PTW 2D-Array (in the following PTW) consists of 729 equally spaced ionisation chambers distributed in an area of 27×27 cm². Each detector covers an area of 5×5 mm² and the measuring depth is at 5 mm water equivalent. The sensitive volume of each chamber is 0.125 cm³. The centre-to-centre distance between two chambers is 10 mm, and a PMMA matrix surrounds the chambers. The chambers have been intercalibrated at the factory to have an equal response within $\pm 2\%$. The electronics is stored in a box, connected through a cable to the device. The data acquisition is done by a laptop

and the whole PTW can be read out every 400 ms [3.51].

a.2.2 Sun Nuclear MapCHECK (MPC)

The Sun Nuclear MapCHECK Model 1175 (MPC) consists of 445 N-type diodes arranged in a 22x22 cm² matrix. Each detector has an active area of 0.8x0.8 mm². The spatial distribution of the diodes is different in the inner part of the matrix with respect to the outer; in the central 10x10 cm² area, diodes are spaced 10 mm along the horizontal and vertical directions and 7.07 mm along the diagonals. In the outer area, diodes are spaced 20 mm along the horizontal and vertical directions and 14.14 mm along the diagonals. Signal processing is done by a personal computer connected through an interface circuit. A dosimetric characterization of MPC can be found in [3.52, 3.53, 3.54]

a.2.3 Torino University/ INFN Pixel Ionization Chamber (PXC)

At the University and Istituto Nazionale di Fisica Nucleare (INFN) of Torino a PiXel-segmented ionisation Chamber (PXC), whose main features are: 2D readout capability, large detection area, good homogeneity and dead time free readout, has been developed in collaboration with Scanditronix-Wellhofer. In brief the PXC consists of a 32x32 matrix of 1024 ionisation chambers arranged in a square of 24x24 cm² area. Each chamber has a 4 mm diameter and 5.5 mm height, the centre at a distance of 7.5 mm from the centre of the next one. The sensitive volume of each single ionisation chamber is 0.07 cm³. The data acquisition system allows an online display rate of 1 Hz, and data storage can be performed at 500?s/reading [3.55, 3.56].

a.3 Accelerators, MultiLeaf Collimators, Treatment Planning Systems

The three 2D verification systems have been tested in the radiotherapy departments of 9 Italian hospitals chosen in such a way that as many as possible configurations of accelerator, delivery and treatment planning system were available. In particular we have used Linac and Multileaf Collimators manufactured by major producers. Both dynamic and step&shoot techniques have been tested. The absolute dosimetry has been performed by each single hospital using the equipment available for patient treatment. Each hospital chose at least 2 fluences, one of which could be considered *typical* and another that had been experienced as *critical* in the dosimetric verification performed before patient treatment. The tests have been performed in the following Hospitals:

- DFC Firenze
- IEO Milano
- IRCC Candiolo
- IRE Roma
- OIRM S.Anna Torino
- REM Radioterapia Catania
- S. Bortolo Vicenza
- S. Giovanni Calibita, Fatebenefratelli, Roma
- S. Maria Nuova, Reggio Emilia

a.4 Results and discussion

The data analysis that we performed on the three detectors had to take into account the different pitches: 7.5 mm for PXC, 10 mm for PTW, and a combination of 5 and 10 mm for MPC. Furthermore the surface of integration is different: a circle of 4 mm diameter for PXC, a square of 5 mm long for PTW, and a square of 0.8 mm long for the MPC. The method for comparing detectors with the same pitch and dimensions would have been immediate. In our case the method had to be more elaborate and three different means of analysis were used, as described below.

Method A consisted of the following steps:

- 1) a line at a distance from the central axis of 10 mm for MPC and PTW and 11.25 mm for the PXC was selected. This choice satisfies two conditions: it is near the central region of the field and minimizes the difference between the MPC and PTW on one side and PXC on the other;
- 2) along this line points were selected for which the absolute distance between the measurement centres of the three detectors was less than 1.25 mm;
- 3) finally those points with a dose larger than 20 % of the maximum dose for that line were selected.

The number of measurement points, N , that were found to match these conditions are reported in Table 1.

For each detector the root mean square (r.m.s) was calculated with respect to the value averaged over the three devices, according to the following relation:

$$\sigma_j = \sqrt{\sum_i \frac{(D_{i,j} - \langle D_i \rangle)^2}{N}} \quad [1]$$

where:

- j runs over PXC to give σ_{PXC} , PTW to give σ_{PTW} , and MPC to give σ_{MPC} ;
- the sum is done over the selected points, N ;
- $D_{i,j}$ is the dose measured for the detector j at point i ;
- $\langle D_i \rangle$ is the average value over the detectors for that point.

$D_{i,j}$ has been obtained by calibrating the array detectors in absolute dose: for the MPC the calibration has been achieved by applying the procedure as established by Sun Nuclear. For the PXC and the PTW the absolute calibration was obtained via a further step, which consisted in comparing them to the MPC for a (10x10) cm² field.

The results are reported in Table 1.

Method B deals with the different geometry of each detector and makes use of the TPS information to compare the results from a single device with the expected dose computed from the TPS output. The original matrices of the various TPS have a pitch between 0.5 and 2.5 mm (reported in Table 2 under column “Pitch”) and this does not allow direct comparison with the matrices obtained from the three detectors. To overcome this problem, all TPS matrices have been transformed into 0.5 mm pitch using a linear interpolation. Once all TPS are in the form of 0.5 mm grid, it is possible to integrate the TPS grid in such a way that the specific geometry of each detector is obtained.

Then the following steps were performed:

- 1) due to the fact that the absolute coordinate system of the TPS with respect to a given detector is not known, a procedure to find the best alignment was implemented. This required finding the minimum sum of the absolute differences between the device response and the computed TPS value by moving the TPS coordinate system in 0.5 mm steps. In this way the problem of different grids for the three detectors was eliminated, allowing the comparison between TPS and measurements;
- 2) to compare the profiles, the r.m.s was computed along a central field line using the following relation:

$$\sigma_j = \sqrt{\sum_i \frac{(D_{i,j} - \langle D_i \rangle)^2}{N}} \quad [2]$$

where all the symbols have the same meaning as in relation [1], $TPS_{i,j}$ is the computed TPS dose in correspondence with point i for detector j , and N is the

number of points with a dose larger than 20% of the maximum dose for the given line.

In Table 2 the results for method B are reported.

Method C makes use of the γ -index calculation. Details on how to compute the index can be found in the literature. Briefly, for each measurement i we computed the following relation:

$$\gamma(r_i) = \min \sqrt{\frac{d^2(r_i, r_{TPS})}{(\Delta d_M)^2} + \frac{\delta^2(r_i, r_{TPS})}{(\Delta D_M)^2}} \quad [3]$$

where d is the distance between r_i , position at which the measurement refers, and r_{TPS} is the TPS position which minimizes the γ function; for Δd_M we used 3 mm. $\delta(r_i, r_{TPS})$ is the difference between the dose at r_i and r_{TPS} , and we used 3% for ΔD_M .

The comparison has been made between each one of the three detectors and the TPS matrices recomputed with 0.5 mm pitch (with the method described above). Only points with a dose larger than 3% of the maximum dose in that field were considered. The 3% cut was increased to 5% when the 3% limit was below 2 cGy.

In Table 3 we report for each detector the number of measurements with $\gamma(r_i) > 1$ and the percentage of points with $\gamma < 1$.

With method A we compared the detectors regardless of the TPS predicted dose distributions. Examining Table 1 we observe that the detector response is within 3% for MPC and PTW for every Centre. The difference between PXC and the other two is somewhat larger and close to 5%. This is in part due to the fact that the centre of the measurements for MPC and PTW coincide, while the PXC detector elements are always displaced by a few millimetres. In one of the Centers (OIRM) the difference is systematically larger: this might be due to the delivered field that was done along a $\pm 20^\circ$ arc.

Method B and C compare the measurements to TPS and they are substantially similar, though B is performed on a more limited region (central) than C. Indeed the two methods gave similar results. In the central region with method B we found an average deviation relative to the maximum delivered dose of: $\sigma_{MPC/\max} = 2.4\%$, $\sigma_{PTW/\max} = 2.0\%$, and $\sigma_{PXC/\max} = 2.8\%$. Responses are almost the same for every Centre?

The results obtained with the first two methods are very similar and show

that despite the difference in accelerator, MLC, and TPS, the three detectors show no substantial differences. More in detail, with Method A, σ (MapCHECK) < 3 cGy in 8/9 hospitals, σ (PTW) < 3 cGy in 8/9 hospitals, σ (PXC) < 3 cGy in 7/9 hospitals where with Method B σ (MapCHECK) < 3 cGy in 8/9 hospitals, σ (PTW) < 3 cGy in 8/9 hospitals, σ (PXC) < 3 cGy in 8/9 hospitals.

Furthermore by examining the results obtained with Method C (γ -index) we note that for both PTW and PXC the percentage of points with $\gamma < 1$ is above 95% in 8 out of 9 hospitals.

For MPC the percentage is somewhat smaller and we interpret this as due to the limited coverage of the field with a high density of diodes. We note that the points with $\gamma > 1$ are mostly confined to areas at the edge of the field and are characterized by low doses, though satisfying the 3% or 5% criteria. Thus the differences in the γ results among the three detectors are mainly limited to low dose points.

Finally the reproducibility of measurements for the three detectors has been measured to be below 0.2 %.

a.5 Conclusions

The use of 2D matrices for IMRT quality assurance has shown to be complementary to film dosimetry. While film is necessary in IMRT commissioning, 2D matrices are well adapted to pre-treatment patient quality assurance, once an IMRT program is completely commissioned. The three detectors that have been tested and reported in this paper are adequate for IMRT verification, also when they are used with different accelerators, MLC and TPS.

Most of the differences between the detectors can be traced back to the geometry, both dimension and location of the detector elements. While PTW and PXC have complete homogenous coverage of the active area, MPC strongly favours the central with respect to the outer region. For this reason the analysis is more complex and the results cannot be compared in a straightforward way.

Hospital	# of points	Sun Nuclear MapCHECK		PTW 2D-Array		Pixel Chamber	
		σ_{MPC} (cGy)	σ_{MPC}/max	σ_{PTW} (cGy)	σ_{PTW}/max	σ_{PXC} (cGy)	σ_{PXC}/max
DFC Firenze	5	2.17	0.021	2.02	0.020	3.52	0.034
IEO Milano	6	1.23	0.028	1.22	0.027	1.31	0.029
IRCC Candiolo	6	1.66	0.058	0.69	0.024	1.83	0.063
IRE Roma	6	1.06	0.019	1.62	0.028	2.36	0.041
OIRM S.Anna Torino	4	2.56	0.113	0.74	0.033	2.12	0.094
S. Bortolo Vicenza	3	4.08	0.029	3.33	0.024	6.15	0.043
S. Giovanni Calibita Roma	8	0.88	0.016	0.87	0.016	1.15	0.021
S. Maria Nuova Reggio Emilia	8	1.00	0.029	0.57	0.017	1.37	0.040

Table 1. Results obtained with Method A for the comparison of the three detectors. The # of points column reports the actual number of points that were used in the comparison (see text for details). The σ_{MPC} , σ_{PTW} , σ_{PX} (cGy) are calculated with the relation [1]. The (σ /max) shows the sigma relative to the max of the line studied.

Hospital	Sun Nuclear MapCHECK		PTW 2D-Array		Pixel Chamber		TPS
	σ_{MPC} (cGy)	σ_{MPC}/max	σ_{PTW} (cGy)	σ_{PTW}/max	σ_{PXC} (cGy)	σ_{PXC}/max	Pitch mm
DFC Firenze	2.08	0.023	1.63	0.015	2.30	0.025	1
IEO Milano	0.43	0.009	1.01	0.019	2.06	0.040	0.5
IRCC Candiolo	1.28	0.046	0.53	0.018	0.96	0.034	2.5
IRE Roma	0.96	0.021	0.68	0.016	1.54	0.035	1.25
OIRM S.Anna Torino	0.72	0.031	0.84	0.034	0.63	0.028	1
REM Catania	2.68	0.023			2.11	0.019	0.5
S. Bortolo Vicenza	4.18	0.026	3.58	0.022	3.65	0.024	1
S. Giovanni Calibita Roma	1.26	0.023	1.32	0.022	1.61	0.027	2.5
S. Maria Nuova Reggio Emilia	0.81	0.017	0.47	0.017	1.05	0.021	2.5

Table 2. Results obtained with Method B for the comparison of the three detectors. The σ (cGy) is calculated with the relation [2]. The (σ /max) shows the sigma relative to the max of the TPS in the line studied that is comparable with the *max* values in each field.

Hospital	Sun Nuclear MapCHECK		PTW 2D-Array		Pixel Chamber	
	# points with $\gamma > 1$	%points $\gamma < 1$	# points with $\gamma > 1$	%points $\gamma < 1$	# points with $\gamma > 1$	%points $\gamma < 1$
DFC Firenze	0	100%	0	100%	0	100%
IEO Milano	4	98%	0	100%	0	100%
IRCC Candiolo	9	92%	0	100%	5	96%
IRE Roma	15	93%	0	100%	11	97%
OIRM S. Anna Torino	9	93%	6	90%	11	90%
REM Catania	1	99%			4	96%
S. Bortolo Vicenza	0	100%	0	100%	0	100%
S. Giovanni Calibita Roma	8	95%	4	97%	5	97%
S. Maria Nuova Reggio Emilia	22	94%	0	100%	21	97%

Table 3. Results obtained with γ -method for the comparison of the three detectors.

References

- 3.1 C Danciu, BS Proimos, JC Rosenwald, BJ Mijnheer "Variation of sensitometric curves of radiographic films in high energy photon beams" *Med Phys* 2001;28(6):966-74.
- 3.2 LJ Bos, C Danciu, CW Chen, MJP Brugmans, A van der Horst, A Minken, BJ Mijnheer "Interinstitutional variations of sensitometric curves of radiographic dosimetric films" *Med Phys* 2002;29(8):1772-80.
- 3.3 JR Sykes, HV James, PC Williams "How much does film sensitivity increase at depth for larger field sizes?" *Med Phys* 1999;26:329-30.
- 3.4 SE Burch, KJ Kearfott, JH Trueblood, WC Sheils, JI Yeo, CKC Wang "A new approach to film dosimetry for high energy photon beams: Lateral scatter filtering" *Med Phys* 1997;29:775-83.
- 3.5 JI Hale, AT Kerr, PC Shragge "Calibration of film for accurate megavoltage photon dosimetry" *Med Dosim* 1994;19:43-46.
- 3.6 JL Robar, BG Clark "The use of radiographic film for linear accelerator stereotactic radio-surgical dosimetry" *Med Phys* 1999;26:2144-50.
- 3.7 IJ Yeo, CKC Wang, SE Burch "A filtration method for improving film dosimetry in photon radiation therapy" *Med Phys* 1997;24:1943-53.
- 3.8 SG, Ju YC Ahn, Huh SJ, Yeo IJ "Film dosimetry for intensity modulated radiation therapy: Dosimetric evaluation" *Med Phys* 2002;29:351-55.
- 3.9 CW Cheng, IJ Das "Dosimetry of high energy photon and electron beams with CEA films" *Med Phys* 1996 ;23 :1225-32.
- 3.10 G Marinello, C Sliwinski. "Les émulsions photographiques et leurs applications en dosimétrie" *J. Radiol. Electrol. Med Nucl* 1974;55:507-14.
- 3.11 B Messerman, C De Wagter "Characteristics of a commercially available film digitizer and their significance for film dosimetry" *Phys Med Biol* 1998;43:1803-12.

- 3.12 JF Dempsey, DA Low, Kirov As, JF Williamson. "Quantitative optical densitometry with scanning-laser film digitizers" *Med Phys* 1999;26:1721-31.
- 3.13 NL Childress, L Dong, II Rosen. "Rapid radiographic film calibration for IMRT verification using automated fields" *Med Phys* 2002;29(10):2384-90.
- 3.14 AJ Olch "Dosimetric performance of an enhanced dose range radiographic film for intensity-modulated radiation therapy quality assurance" *Med Phys* 2002;29(9):2159-68.
- 3.15 XR Zhu, PA Jursinic, DF Grimm, F Lopez, JJ Rownd, MT Gillin "Evaluation of Kodak EDR2 film for dose verification of intensity modulated radiation therapy delivered by a static multileaf collimator" *Med Phys* 2002;29(8):1687-92.
- 3.16 J Esthappan, S Mutic, WB Harms, JF Dempsey, DA Low "Dosimetry of therapeutic photon beams using an extended dose range film" *Med Phys* 2002;29(10):2438-45.
- 3.17 N Dogan, LB Leybovich, A Sethi "Comparative evaluation of Kodak EDR2 and XV2 films for verification of intensity modulated radiation therapy" *Phys Med Biol* 2002;47(22):4121-30.
- 3.18 M Bucciolini, F Banci Buonamici, M Casati "Verification of IMRT fields by film dosimetry" *Med Phys* 2004;31(1):161-8.
- 3.19 C Martens, I Claeys, C De Wagter, W De Neve "The value of radiographic film for the characterization of intensity-modulated beams" *Phys Med Biol* 2002;47:2221-3.
- 3.20 N Agazaryan, TD Solberg, JJ DeMarco "Patient specific quality assurance for the delivery of intensity modulated radiotherapy" *J Appl Clin Med Phys* 2003;4(1):40-50.
- 3.21 DA Low, WB Harms, S Mutic, JA Purdy "A technique for the quantitative evaluation of dose distribution" *Med Phys* 1998;25:656-61.
- 3.22 T Depuydt, A van Esch, DP Huyskens. "A quantitative evaluation of IMRT dose distributions: refinement and clinical assesment of the gamma evaluation" *Radiother Oncol* 2002;62:309-19.
- 3.23 L Dong, J Antolak, M Salehpour, K Forster, L O'Neill, R Kendall, I Rosen "Patient-specific point dose measurement for IMRT Monitor Unit verification" *Int J Radiat Oncol Biol Phys* 2003;56(3):867-77.
- 3.24 M Casati "Dosimetria Fotografica nella Radioterapia a Modulazione di Intensità" Unpublished thesis, Florence University, 2003
- 3.25 PA Jursinic, BE Nelm "A 2-D diode array and analysis software for verification of intensity modulated radiation therapy deliver" *Med Phys* 30(5);2003:870-9.
- 3.26 J van Dyk, RB Barnett, JE Cygler, PC Shragge "Commissioning and Quality Assurance of Treatment Planning Computers" *Int J Radiat Oncol Biol Phys* 1993;26:261-73.
- 3.27 DA Low, WB Harms, S Mutic, JA Purdy "A technique for the quantitative evaluation of dose distributions" *Med Phys* 1998;25(5):656-61.
- 3.28 DA Low, JF Dempsey "Evaluation of the gamma dose distribution comparison method" *Med Phys* 2003;30(9):2455-64.
- 3.29 T Depuydt, A Van Esch, DP Huyskens "A quantitative evaluation of IMRT dose distributions: refinement and clinical assessment of the gamma evaluation" *Radiother Oncol* 2002;62:309-19.
- 3.30 IJ Yeo, A Beiki-Ardakani, Y Cho, M Heydarian, T Zhang, M Islam "EDR2 film dosimetry for IMRT verification using low-energy photon filters" *Med Phys* 2004;31(7):1960-3.
- 3.31 LB Leybovich., A Sethi, N Dogan "Comparison of ionization chambers of various volumes for IMRT absolute dose verification" *Med Phys* 2003;30(2):119-123

- 3.32 M Stasi, B Baiotto, G Barboni, G Scielzo "The behavior of several microionization chambers in small intensity modulated radiotherapy fields" *Med Phys* 2004;31(10):2792-2795.
- 3.33 D Létourneau, M Gulam, D Yan, M Oldham, JW Wong "Evaluation of a 2D diode array for IMRT quality assurance" *Radiotherapy and Oncology* 70(2004), 199-206.
- 3.34 MC Kirby, PC Williams, "The use of an electronic portal imaging device for exit dosimetry and quality control measurements," *Int. J. Radiat. Oncol., Biol., Phys.* 31, 593-603 (1995).
- 3.35 K L Pasma, M Kroonwijk, JCJ de Boer, AG Visser, BJM. Heijmen., "Accurate portal dose measurement with a fluoroscopic electronic portal imaging device (EPID) for open and wedged beams and dynamic multileaf collimation," *Phys. Med. Biol.* 43, 2047-2060 (1998).
- 3.36 S N Boon, P van Luijk, T Böhringer, A Coray, A Lomax, E Pedroni, B Schaffner, JM Schippers, "Performance of a fluorescent screen and CCD camera as a two-dimensional dosimetry system for dynamic treatment techniques," *Med. Phys.* 27, 2198-2208 (2000).
- 3.37 Y Zhu, XQ Jiang, J Van Dyk, "Portal dosimetry using a liquid ion chamber matrix: dose response studies," *Med. Phys.* 22, 1101-1106 (1995).
- 3.38 H Parsaiea, E El-Khatib, R. Rajapakshe, "The use of an electronic portal imaging system to measure portal dose and portal dose profiles," *Med. Phys.* 20, 1903-1909 (1998).
- 3.39 M Essers, R Boellaard, M van Herk, H Lanson, B Mijnheer, R Rajapakshe, "Transmission dosimetry with a liquid-filled electronic portal imaging device," *Int. J. Radiat. Oncol. Biol. Phys.* 34, 931-941 (1996).
- 3.40 H Keller, M Fix, P Ruegsegger "Calibration of a portal imaging device for high-precision dosimetry: a Monte Carlo study" *Med. Phys.* 25, 1891-1902 (1998).
- 3.41 BMC McCurdy, K Luchka, S Pistorius "Dosimetric investigation and portal dose image prediction using an amorphous silicon electronic portal imaging device" *Med. Phys.* 28, 911-924 (2001).
- 3.42 A Van Esch, T Depuydt, and DP Huyskens "The use of an a Si-based EPID for routine absolute dosimetric pre-treatment verification of dynamic IMRT fields" *Radiother. Oncol.* 71, 223-234 (2004).
- 3.43 CV Dahlgren, K Eilertsen, TD Jørgensen, A Ahnesjö "Portal dose image verification: the collapsed cone superposition method applied with different electronic portal imaging devices" *Phys. Med. Biol.* 51, 335-349 (2006).
- 3.44 R Boellaard, M van Herk, BJ Mijnheer "A convolution model to convert transmission dose images to exit dose distributions" *Med. Phys.* 24, 189-199 (1997).
- 3.45 S Steciw, B Warkentin, S Rathee, BG Fallone "Three-dimensional IMRT verification with a flat panel EPID" *Med. Phys.* 32, 600-612 (2005).
- 3.46 M Partridge, M Ebert, B. M. Hesse "IMRT verification by three-dimensional dose reconstruction from portal beam measurements" *Med. Phys.* 29, 1847-1858 (2002).
- 3.47 J Chang, GS Mageras, CC Ling, W Lutz "An iterative EPID calibration procedure for dosimetric verification that considers the EPID scattering factor" *Med. Phys.* 28, 2247-2257 (2001).
- 3.48 BMC McCurdy, S Pistorius "A two-step algorithm for predicting portal dose images in arbitrary detectors" *Med. Phys.* 27, 2109-2116 (2000).
- 3.49 B Warkentin, S Steciw, S Rathee, BG Fallone "Dosimetric IMRT verification with a flat-panel EPID" *Med. Phys.* 30, 3143-3155 (2003).
- 3.50 WD Renner, K Norton, T Holmes "A method for deconvolution of integrated electronic portal images to obtain incident fluence for dose reconstruction" *J. Appl. Clin. Med. Phys.* 6,

22-39 (2005).

- 3.51 E Spezi, AL Angelini, F Romani, A Ferri “Characterization of a 2D ion chamber array for the verification of radiotherapy treatments” *Phys Med Biol* 50: 3361-3373; 2005.
- 3.52 JG Li, JF Dempsey, L Ding, C Liu, JR Palta “Validation of dynamic MLC-controller log files using a two-dimensional diode array” *Med Phys* 30: 799- 805; 2003.
- 3.53 PA Jursinic, BE Nelms “A 2-D diode array and analysis software for verification of intensity modulated radiation therapy deliver” *Med Phys* 30: 870-879; 2003.
- 3.54 D Letourneau, M Gulam, D Yan, M Oldham, JW Wong “Evaluation of a 2D diode array for IMRT quality assurance” *Radiother Oncol* 70: 199-206; 2004.
- 3.55 S Amerio, A Boriani, F Bourhaleb, R Cirio, M Donetti, A Fidanzio, E Garelli, S Giordanengo, E Madon, F Marchetto, U Nastasi, C Peroni, A Piermattei, CJ Sanz Freire, A Sardo, E Trevisiol “Dosimetric characterization of a large area pixel segmented ionization chamber” *Med Phys* 31: 414-420; 2004.
- 3.56 M Stasi, S Giordanengo, R Cirio, A Boriani, F Bourhaleb, I Cornelius, M Donetti, E Garelli, I Gomola, F Marchetto, M Porzio, CJ Sanz Freire, A Sardo, C Peroni “D-IMRT verification with a 2D pixel ionization chamber: dosimetric and clinical results in head and neck cancer” *Phys Med Biol* 50: 4681-4694; 2005.

4. Dose calculation and plan optimisation: computational and radiobiological aspects in IMRT

4.0 Sommario

L'obiettivo di questo capitolo è quello di fornire una panoramica sulle problematiche della fisica computazionale nel settore della IMRT.

Ci sono due aspetti della radioterapia che necessitano di una modellistica di tipo fisico-matematico [4.1]: il calcolo della dose e la ricerca di una distribuzione di dose quanto più vicina possibile a quella prescritta dal medico radioterapista (problema inverso).

Il calcolo della dose può essere effettuato utilizzando algoritmi simili a quelli impiegati nella radioterapia convenzionale; occorre però tenere in considerazione che, nell'impiego delle tecniche ad alto grado di conformazione, è necessaria un'elevata precisione nel calcolo della dose. In IMRT le dosi vengono calcolate dividendo i fasci di trattamento in piccole sezioni chiamate "beamlet". Con fasci di piccole dimensioni come i beamlet, l'equilibrio elettronico non viene necessariamente garantito per cui gli algoritmi di calcolo, che fanno uso di fasci convenzionali, potrebbero portare ad errori consistenti nel calcolo della dose. Metodi di calcolo più accurati (pencil beams o kernel di dose) o l'utilizzo di tecniche come il Monte Carlo rappresentano una scelta più adeguata per il calcolo della distribuzione di dose, anche se spesso i lunghi tempi di calcolo ne limitano l'utilizzo nella pratica clinica [4.4].

Nell'ambito di ciò che viene definito problema inverso è necessario determinare un modello di "beamlet intensities" per ogni campo definendo una funzione costo, che rappresenta una misura della distanza tra la distribuzione di dose prescritta e quella ottenuta. Un opportuno metodo di minimizzazione (processo di ottimizzazione) permetterà di ottenere il minor scarto tra le due distribuzioni anche se la pianificazione inversa non produce, in modo automatico, la migliore distribuzione di dose, ma una soluzione che dipende dai vincoli sulla e dalla definizione della stessa funzione costo.

Infine, la valutazione dei risultati ottenuti nel processo di ottimizzazione devono essere valutati in base ad un approccio interdisciplinare basato sulle conoscenze fisiche, radiobiologiche e cliniche.

Questo capitolo si articola in due sezioni. La prima riguardante il problema del calcolo della dose e gli aspetti computazionali legati alla pianificazione inversa del trattamento e quindi alla fase di ottimizzazione del tratta-

mento, da un punto di vista fisico-matematico.

La seconda analizza, in modo sintetico, la modellizzazione radiobiologici di *TCP* (Tumour Control Probability) ed *NTCP* (Normal Tissue Complication Probability). Questi indicatori radiobiologici non permettono di ottenere previsioni individuali affidabili, sull'esito della terapia o sulle tossicità associate, a causa delle ampie incertezze che affliggono i valori dei parametri radiobiologici da essi usati (ad esempio α , α/β , rapidità proliferativa, densità clonogenica iniziale, grado di serialità e parallelismo di un organo). Tuttavia, tali modelli radiobiologici sono stati proficuamente utilizzati in letteratura per confronti sia tra diversi schemi di frazionamento che tra differenti tecniche d'irraggiamento, con e senza modulazione di fascio. Adottando questa prospettiva di utilizzo in senso 'relativo' della modellizzazione radiobiologica, sono stati affrontati due tra gli aspetti specifici del trattamento IMRT: l'abilità del fascio modulato di 'scolpire' la dose su possibili focolai intratumorali di elevata radioresistenza o attitudine proliferativa, e l'esigenza di una caratterizzazione biologica delle funzioni costo alla base dell'ottimizzazione delle matrici di fluena.

4.1 Introduction

Implementation of IMRT needs important changes in treatment planning strategies, and it is crucial that an interdisciplinary effort is made to integrate sophisticated mathematical models and advanced computing knowledge into the treatment planning process and to investigate cutting edge methods of optimizing the clinical outcome of radiotherapy.

As described by Censor [4.1], there are two aspects of radiation therapy that call for mathematical modeling: the calculation of the radiation dose (the "forward problem" of IMRT) and the definition of the radiation intensity function (the solution of the "inverse problem"), as similar as possible to the desired dose function prescribed by the radioterapist.

Simple IMRT planning can be accomplished by manually adding subfields with various weights and evaluating the dose distribution. In each iteration of the process, the planner decides what changes to make to revise the design. The planning process is not automated and is called forward planning. This method typically produces a limited number of subfields and is a natural evolution of 3-D conformal planning. Another approach to IMRT planning breaks each beam into many small beamlets and determines the intensity of each [4.12]. Having a large number of segments or beamlets makes the problem of determining individual intensities very complex and

requires computerized methods for solution (inverse planning). The planner specifies beam directions and/or arc angles, target dose goals, and dose constraints or goals for sensitive structures, and then an automated optimization algorithm calculates intensity patterns that create a dose distribution that best meets the prescription.

The calculation of the radiation dose can be performed by using algorithms similar to those used in traditional radiotherapy (e.g. pencil beam dose calculation) or Monte Carlo methods [4.4]. Monte Carlo algorithms may play an important role in IMRT because a higher level of accuracy is desirable, reduced margins are often used and dose gradients may be steep near critical structures [4.42].

The inverse planning systems must determine a pattern of beamlet intensities for each field and translate it to delivery instructions for the system being used. The inverse problem is solved by defining a cost function, that is a measure of the distance between the desired dose and the obtained one, to be minimized by a suitable method.

The inverse treatment plan will not automatically generate an optimum dose distribution, but a solution that is dependent on the dose constraints and objective function specified by the user. An interdisciplinary approach is necessary to evaluate the results obtained in the optimization process based on physical, radiobiological and clinical knowledge.

4.2 Dose calculation algorithms for IMRT

IMRT differs from 3D-CRT in two major aspects: the use of numerical optimization methods to achieve prescription goals and the leaf motion calculators used to determine a sequence of radiation fields, which vary in shape and in the number of monitor units (MUs) applied. It is important to recognize how these components interact with the more familiar components of the planning system, including heterogeneity corrections, but the dose calculation models used are similar to those used in 3D-CRT. In fact, the distribution dose conformation is realized by considering the beam as formed by several small beams of square shape and millimeter dimensions (beamlets). For each beamlet the dose distribution is calculated using algorithms similar to those used for the conventional conformal radiotherapy. Finally, the required dose distribution is obtained by the optimization algorithms that calculate the single beamlet relative weight using its dose distribution. The IMRT planning is more time consuming with respect to the 3D-CRT because of large number of degrees of freedom in the same treatment planning.

The IMRT dose distributions can be calculated by using three different types of algorithms: correction-based, model-based [4.3] and direct Monte Carlo. The model-based algorithms and the direct Monte Carlo are becoming more and more the algorithms of the future, because of their ability to simulate radiation transport in three dimensions and therefore, more accurately predict dose distribution under conditions of charged particles disequilibrium, which can occur in low-density tissue and heterogeneous tissue interface.

The correction-based algorithms are semi-empirical. In the correction-based algorithm, the dose distribution in the patient is described by several experimental parameters. These are initially obtained by measuring the beam characteristics in a water phantom and then corrected in order to take into account patient geometry. The accuracy of these algorithms is limited for 3-D heterogeneity corrections in low-density tissue and tissue interface especially in situations where electronic equilibrium is not fully established.

A model-based algorithm computes the dose distribution with a physical model that simulates the actual radiation transport. The set up of the model-based algorithm requires less measured data than the correction-based models. Furthermore, the dose distribution in the patient is directly calculated taking into account the geometry, the energy, the beam modifiers, the ROI and the tissue heterogeneities. The convolution/superposition algorithms [4.5, 4.6, 4.7] are classified as model-based algorithms.

In the convolution/superposition algorithms the dose deposition is considered as kernels [4.8, 4.9, 4.10, 4.11, 4.13] superposition. Each kernel, which describes the energy transport and the dose deposition of the secondary particles originating from an irradiation point, is suitably weighted in the irradiation points. When the kernels are spatially invariant the superposition can be evaluated by the convolution. The kernels can be calculated by Monte Carlo method.

The model-based algorithms, taking into account the lack of electronic equilibrium, are more accurate than correction-based algorithms in the dose calculation especially in the electronic disequilibrium and heterogeneous regions.

Most IMRT implementations use fast pencil beam algorithms (less than 1 second to compute dose distribution for a beam) to compute dose. These methods use the effective radiological path-length correction to account for heterogeneities.

The above reported considerations show that all algorithms approximate

the real physical situation. As a result of these approximations, the model generally contains uncertainties limiting the application in clinical cases. Therefore, a quality assurance of treatment planning software is required to reduce uncertainties in the treatment planning process.

4.3 Monte Carlo algorithms in IMRT: some features

The Monte Carlo algorithms have been proven to be a realistic alternative to analytical algorithms. Monte Carlo can provide dose calculation map with the high level of accuracy required by IMRT. The result of the simulation is influenced by two kind of parameters: the physical description of the interaction of radiation with matter and the representation of the radiation source including beam modifiers.

The characteristics of the accelerators are generally obtained from the commercial manufacturers. While, the description of the initial beam can not be known with the desired accuracy since every electron accelerator is usually fine-tuned after installation [4.14]. The source parameters may be defined iteratively: first of all it is necessary to choose a set of initial parameters (e.g. from the literature), then to run the simulation. Hence on the basis of the results obtained (percentage depth dose (PDD), output factor (OF) and beam dose profiles) it is possible to tune the set of parameters until obtaining the desired agreement. The initial electron beam is usually described as double-differential distribution of lateral fluence in energy and direction. Modern linear accelerators have a Gaussian lateral distribution with a 1-3 mm full width maximum height (FWMH) [4.15, 4.17, 4.18, 4.19] and a squared scattering angle of about 0.003 rad^2 [4.20].

The energy distribution of electron beam depends essentially on: acceleration type (traveling or standing wave), electron injection method, wave guide tuning, beam handling system and steering magnet. Recently, however, it has been shown that the dose distribution is not so heavily dependent on the description of the initial electron beam [4.21]. If the initial spectrum is symmetric and with a FWHM smaller than 10% of the medium energy of the beam, the energy spectrum poorly affects the lateral dose profile and the influence on PDD is negligible.

Once the characterization of the accelerator beam is done, it is possible to obtain a detailed description of the phase space of the particles below the jaws. In IMRT it is also relevant to describe the secondary ML collimation. A frequently used approach is to directly use the treatment planning system's intensity matrix (IM) (or a similarly produced IM) to account for intensity

modulation during the simulation, i.e., use the same intensity matrix to modulate the incident particle stream as the one used for the non-Monte Carlo IMRT dose calculations. While the IM method is extremely fast for Monte Carlo, it is also overly simplistic because it effectively accounts only for the patient heterogeneities and not for the incident fluence prediction. It may therefore have only a modest accuracy advantage over superposition convolution algorithms. The weakness of the IM approach is that it does not account for scattered photons and electrons produced in the MLC. To account for MLC leaf leakage an empirical correction term can be introduced [4.5]. However, this neglects the energy and angular dependence of the scattered radiation. The most rigorous method of Monte Carlo use for calculating dose distributions for intensity-modulated fields is the direct use of the leaf-sequence file and leaf positions during the radiation transport simulation. There are numerous published examples of modeling MLCs for Monte Carlo calculations [4.14]. However, as mentioned above, detailed transport through the full MLC geometry is computer-time prohibitive. To increase the dose-calculation speed, simplifying geometric assumptions are usually made. For example, DMLC-IMRT fields may be simulated as a sequence of many (hundreds of) static fields. Other geometric simplifications include ignoring details of the leaf sides or including the leaf edges but approximating the rounded MLC leaf tip with a focused leaf tip with an effective offset [4.22]. A good example of a IMRT treatment simulation can be found in [4.23].

The most severe obstacle to the clinical application of Monte Carlo methods to the clinical routine is the computational load needed for the dose calculation and the skill and know-how required to run the actual codes. A possible solution is to run a complete IMRT treatment simulation on a cluster of off-the-shelf PC, so reducing the time required for dose calculation [4.24].

4.4 IMRT optimization

IMRT planning is characterized by a huge number of parameters such that the optimal beam configuration, suited for producing the desired dose distribution on the target and organs at risk, cannot be achieved through the “trial and error” method typically applied in conventional radiotherapy [4.1]. The most common approach to determine the best intensity modulation is based instead on heuristic methods.

In inverse planning, the user specifies objectives for the dose distribution using single dose value, a few dose–volume points, or fully flexible DVHs. Importance factors may be used to change the relative weight given to different objectives. Internally, the planning system represents these objectives

in a cost function, which must be minimized by an optimization algorithm. The cost function numerically attempts to represent the tradeoffs that are incorporated into clinical judgment. By changing the objectives, the user alters the cost function and so influences the result.

Then, the cost function represents the “error” associated to the treatment plan obtained and quantifies how much a particular intensity modulation is close to the optimal choice. So the best beam modulation minimizes the cost function. Given a cost function, the optimization problem becomes the search for the minimum of such a function, that can be found by using a suitable optimization algorithm. In a radiotherapy context the treatment parameters define the search space.

Optimization algorithms used to minimize the cost functions can be classified into two broad categories: deterministic and stochastic. Deterministic methods move from one proposed solution to the next using computed first and/or second derivatives of the cost function. The direction and size of each step i.e., which beamlet intensities change and by how much, depends on the computed gradients. Minimization can be relatively fast but cannot escape from a local minimum. Stochastic methods move from one proposed solution to the next by randomly changing beamlet intensities according to some scheme. Because disadvantageous changes are sometimes allowed, escape from local minima is possible. Simulated annealing is one stochastic technique that has been adapted to IMRT.

Webb [4.25] and Bortfeld [4.26] affirm that a simple quadratic cost function, based on the summed squares of the pixel-by-pixel differences between desired and actual doses, has not local minima, if one chooses to optimize the beam intensities but not beam orientations. But if we choose to incorporate constraints on dose levels inside each region of interest (ROI) in the cost function definition (DVH-based cost function) we can observe multiple minima. In this case the optimization process becomes complex and time consuming so it is necessary to adopt different minimization strategies, able to escape from local traps and to reach the global minimum. For this reason many other algorithms have recently been implemented, based on stochastic procedures, to ensure a correct treatment planning optimization.

4.5 Cost Function definition

A given cost function can be optimized using a number of different optimization algorithms, such as iterative approaches, simulated annealing, filtered backprojection, etc.

The optimization process could be visualized as the “motion” of a point representing the modulation profile, on the surface describing a ‘cost function’ $F(x)$, whose value at each point encodes the “penalty” for being non-optimal (see for instance [4.27]). The best modulation profiles are then identified with the minimum (or minima) of $F(x)$. The cost function is defined in a space having as many dimensions as the number of pencil beams; therefore it is a high dimensional space, something to be kept in mind when exercising intuition on the process.

Cost function encapsulates the clinical objectives of the treatment plan, and its definition represents a critical point of the optimization process. It can be based on dose-based criteria (physical cost function), or on biological criteria (biological cost function). Biological cost function represents a more clinically relevant approach, because it makes it possible to predict the radiation effects on tissues and so to estimate the final efficacy of the therapy (see Chapter on “Aspects of radiobiological modelling in IMRT”). A biological cost function can be considered more efficient than a dose/volume cost function only if the parameters of the radiobiological models are known with accuracy better than the typical one. Consequently, it is necessary to collect clinical data regarding outcome, with an accurate description of the irradiation geometry, dose distribution in the tumour and in organs at risk. In the absence of radiobiological data the use of a more reliable physical cost function is preferable.

The simplest dose-based cost function consists of a quadratic difference between the desired dose distribution and the actual one inside each region of interest [4.28, 4.29]. Actually, dose-volume objective function is the most significant way to approach the optimization problem in IMRT because it provides more flexibility for the optimization process and greater control over the dose distribution [4.30, 4.31]. This type of function is based on the results of the dose-volume histogram (DVH) analysis of the treatment plan. The analysis of the DVH provides the most common tool to evaluate the quality of a treatment plan, since it shows a synthesis of the dose distribution over the volumes involved.

Constraints on the dose delivered inside each region of interest (ROI) are taken into account in order to maximize the dose level and homogeneity in the target with minimal damage to normal tissues and organs at risk (OARs). They are explicitly incorporated in the model and can be expressed through dose-volume limits, defined as the maximum volumes that have not received

a dose greater than given tolerance values.

4.6 Minimization: a search for the best treatment plan

Due to the strong non-linearity of the system and to the large number of dimensions of the configuration space for the IMRT (pencil beam numbers composing the intensity maps, the number of beams involved in the treatment, the possible energies of the used fields, etc.), a heuristic approach is required to locate the global minimum. Analytical approaches can be devised only in strongly simplified situations, typically in non realistic clinical conditions [4.28].

One of the difficulties in the minimization is the convergence problem. In fact the heuristic algorithm may not reach in a reasonable finite time the optimal solution for at least two reasons: i) it may be trapped in local minima (sub-optimal solutions); ii) the “motion” on the surface $F(x)$ may become slow or oscillating in a region of the configuration space.

The issue related to local minima in IMRT treatment planning have been addressed in recent literature [4.2, 4.32]. The conditions for the existence of local minima have been investigated; in particular it has been recognized that the choice of dose-volume constraints implies local minima in the cost functions [4.31, 4.33], as opposed to the quadratic cost function [4.25]. Furthermore, in more realistic conditions [4.27, 4.34, 4.35, 4.36, 4.37], the existence of local minima has been confronted using the “configuration space analysis” [4.38]. The method consists of following the trajectory of many minimization processes starting from randomly chosen initial plan configuration: if the algorithm used is not able to escape from local minima the distribution of sub-optimal solutions in the parameter space emerges. As a general result a rich pattern of local minima is found also for a radiation therapy approach different from IMRT. To find good solutions in the presence of sub-optimal TP, several stochastic algorithms have been proposed [4.28, 4.39]. However, to have solutions close to the optimal one, high computational load is necessary. On the other hand some recent results question the relevance of the pattern of local minima [4.30, 4.33, 4.35, 4.37]. A natural question then arises: how much does the optimization have to be refined in order to provide a good enough TP? Are sub-optimal solutions qualitatively different from the optimal one? Is it necessary to choose a “smart” heuristic, resulting however in a strong computational load, to have a qualitatively reasonable result? To answer this question the optimization process has to be evaluated. A possible way to evaluate the optimization process is reported in [4.27, 4.35, [4.40]. The impact of the complexity of the optimization process may also be eval-

uated making the connection between the variability due to the pattern of local minima and the actual precision (and reproducibility) with which a prescribed IMRT modulation profile can be implemented by the multi-leaf system [4.41], since this sets the scale below which any differences in sub-optimal solutions are ineffective.

4.7 Aspects of radiobiological modelling in IMRT

The high conformality of IMRT plans, characterized by steep dose gradient regions all around the tumour, make them highly sensitive to treatment uncertainties which come from set-up error and organ motion [4.43, 4.44]. Furthermore, IMRT plans typically associate inhomogeneous dose distributions with the organs at risk (OAR) adjacent to the tumour. Several dose-volume histogram reduction schemes were proposed to convert an inhomogeneous dose distribution into an equivalent uniform irradiation [4.45], however firstly our present knowledge of OAR's toxicities is limited to standard fractionation (~2 Gy, once daily 5-days-per-week), secondly it antedates CT-treatment-planning [4.46] and thirdly there are low-rates of complications. It may therefore turn out to be at least partially unsuitable for IMRT.

These characteristics of IMRT make it necessary to use well defined biological criteria for treatment planning and to correlate them with clinical outcomes. Insecurity with Tumour Control Probability (*TCP*) and Normal Tissue Complication Probability (*NTCP*) models, due to their simplistic approach and the lack of reliable in vivo response data, has limited their use for clinical predictions up to now. However, "dose and dose-volume indices are even more simplistic measures of the quality of the optimized treatment plan" [4.47]. Furthermore some uses of radiobiological modelling, e.g. to evaluate the impact of inter- and intra-observer variability in contouring the regions of interest [4.48] or to look for the optimized treatment schedule [4.49, 4.50], have gained general acknowledgement.

The present brief review has thus been devoted to some specificities of IMRT, such as its dose sculpting ability to and within the tumour and its need for objective functions as a guide for inverse planning, which are strictly determined by the level of comprehension of the radiobiology of both tumour and normal tissue. Once a multiplicity of tumour foci of different radiobiology are identified within the tumour by means of functional imaging, biological optimization will be needed to sculpt the optimal inhomogeneous dose distribution. The biological objective function will then be constructed around those predictive variables obtained from functional imaging which will better correlate with clinical outcome, on the basis of prospective stud-

ies in large patient populations.

4.7.1 Biological conformality

The dose sculpting ability of IMRT for spatially customize 3D-dose delivery to supposed tumour foci of increased radioresistance or proliferative capabilities, has been proposed as a possible rationale for the adoption of such a technique.

Reviews of the presently available radiobiological imaging which ought to give information on such factors as tumour hypoxia or proliferative capabilities are given in [4.51, 4.52], with main reference to nuclear medicine (PET) and magnetic resonance spectroscopy (MRS). Fluoromisonidazole (^{18}F -Miso) [3.53] and the copper chelate Cu-ATSM [3.54] as hypoxic PET-tracers, Fluorodeoxyglucose (^{18}F FDG) as PET-tracer for increased metabolic activity, and choline/citrate ratio as ^1H -MRS-marker for increased cell proliferation [4.55] may be cited amongst the most debated functional imaging techniques.

Using the LQ-model including repopulation, but with limited reference to slowly-proliferating tumours, Tomè and Fowler [4.56] show how a significant gain in TCP may be derived from dose boost ratios as low as (1.2 ÷ 1.3) if encompassing tumour volume fractions as large as (60% ÷ 80%). Rather than suggesting tumour dose sculpting, this seems to be a rationale for dose-escalation to almost the whole tumour volume. In their study Tomè and Fowler describe the intra-tumour heterogeneity in radiosensitivity ($SF_2 = \exp(-2\alpha-4\beta)$) by normal distribution: such radiosensitivity is then not voxel-indexed, neither any explicit reference to spatially well-defined radioresistant sub-volumes (as suggested in [4.51]) is made.

This issue has been outlined by Deasy in a short note [4.57] where he hypothesizes, within a spatially simple but instructive model for the intra-tumour α -heterogeneity (single radioresistant-voxel), that the expected gains from partial tumour dose boosts described in [4.56] might have been underestimated. If a gain in TCP around (10 ÷ 15)% over the 50% baseline had been associated in [4.56] to boosted fractional tumour sub-volumes not smaller than (60 ÷ 80)%, the same TCP gain for the same dose boost ratio (= 1.2) is now computed for about (30 ÷ 50)% fractional sub-volumes.

For a spherical tumour symmetry, both a linear and an exponential variation with distance r from tumour centre for both the radio sensitivity, $\alpha(r)$, and the repopulation rate, $\gamma(r) = \ln 2 / T_{pot}(r)$, have been considered in the mathematically detailed model proposed by Levin-Plotnik and Hamilton [4.58].

However contradictory results may be deduced about the optimal spatial dose distribution according to the balance between the intra-tumour distributions for radioresistance and repopulation. The matter is thus becoming complex: perhaps no single functional imaging can guide the dose sculpting to the tumour, which should rather arise from the integration of both radiosensitivity and repopulation mappings.

Last but not least, the time-modulation of such $\alpha(\mathbf{r})$ and $\gamma(\mathbf{r})$ -mappings ought to be included. The impact of the temporal variability of the spatial location of the acutely hypoxic tumour clonogens, $\alpha(\mathbf{r},t)$, on the estimated *TCP*, although neglecting the effect of clonogenic proliferation, has been modelled by Popple et al. [4.59]. The relative *TCP* gain now seems crucially dependant on the acutely hypoxic fraction or, in the authors' words, "when the hypoxia is primarily transient, a boost dose does not significantly improve the *TCP*" whereas when the hypoxia is geometrically stable (chronic) "the *TCP* increases significantly for relatively modest boost doses to the hypoxic volume" even if this is not completely encompassed in the boost.

Therefore, when dealing with tumour hypoxia it should be significant, not only to get a radiobiological measure of it as a whole, but also to quantify its partition into the acutely and the chronically hypoxic fractions. To date, only the oxygen microelectrode method has proved to assure pre-treatment measures of tumour oxygenation that correlate with local control and disease-free survival [4.60], whereas an indirect estimate of the acutely hypoxic fraction from successive binding of both proliferative (IdUrd) and hypoxic (pimonidazole) immuno-histochemical markers has been reported [4.61]: however these data are not useful for co registration to CT images aiming at functional-image guided IMRT.

However, some useful suggestions may be deduced from such analysis. First, the magnitude of the optimal dose boost ratio, as suggested in [4.62] and [4.59], seems much lower than that usually applied in other highly conformal techniques (e.g. brachytherapy). In addition, multiple sources of radiobiological imaging dealing with at least radio sensitivity and repopulation, repeated over the treatment period to account for vascular tumour remodelling, seem necessary to guide dose painting.

However, to our knowledge, no general consensus on any specific marker for total hypoxia has been found, nor is functional imaging able to distinguish between acute and chronic hypoxia at present. Much work remains to be done to determine how graded levels of metabolic activity can be used to guide the graded levels of dose delivery by IMRT. These kinds of biological

link to the functional image-guided IMRT chain remain therefore the weakest one: nevertheless, it seems reasonable to direct the hot-spots so frequently generated by the optimisation algorithms towards regions of supposed increased radio resistance or proliferate activity.

4.7.2 Biological objective functions

A few papers, although increasing in frequency, have described how optimization of the biophysical objective functions produces a therapeutic benefit compared to physical objective functions alone [4.47, 4.62, 4.63]. The more appealing aspect is the possibility of exploring a wider range of dose distributions, because there are many (infinite) dose-volume histograms (DVH) that lead to the same dose response. Constraining the optimization to particular DVH limits, the search for the best intensity modulation, instead a biological optimization gives greater flexibility to the minimization process. Another point is that if a small part of the tumour receives a very low dose, it would not have an evident effect on the DVH and so on the plan, while the *TCP* would be greatly decreased by the presence of cold spots. On the contrary, it has also been concluded that the use of biological objective function needs the addition of physical constraints to avoid large target dose inhomogeneity (especially high dose values).

Now we briefly summarize some examples of biological objective functions. A simple form is the following:

$$F = TC^c \cdot \prod_i (1 - NTCP_i)$$

where F represents the uncomplicated control probability and $NTCP_i$ refers to the i -th OAR. The parameter c has been introduced to increase the weight of *TCP* with respect to the complication probabilities. Another mathematically correct form may be:

$$F = TC^c \cdot \prod_i w_i (1 - NTCP_i)$$

where the weighting factors are transferred to the OARs. It is not straightforward to specify the appropriate values for w_i , which depend on the clinical situation (prostate, head and neck ...), on the different effect of toxicities on the quality of life, taking into consideration patient survival probability. Thus, the definition of the biological objective function is a hard task but some anomalies, such as an undesired target dose inhomogeneity, can be overcome. In particular it is important to correctly normalize the plan at the end of the optimization, because this can lead to a different optimal solution of the objective function. The w_i values depend upon the beam orientation scheme also, which strongly affects the role of the surrounding OARs to limit

the dose to the target.

A more recent model [4.47] is based on the equivalent uniform dose (*EUD*), which was defined as the dose that, if given uniformly, should lead to the same surviving fraction as the actual non-uniform dose distribution [4.64].

A former study by Ebert [4.65] showed that *EUD* provides a reliable dose indicator, stable and less sensitive to the α/β value and to population averaging than *TCP*. So, *EUD*, which represents a dose and does not predict the biological response, “can bridge the gap between the obvious limitations of dosimetric based optimization and the more appealing [4.68] methods of biologic based optimization”, without requiring full knowledge of radiobiological models [4.66].

A novel approach to the objective function modelling has been proposed by Xing [4.67], which integrates into the mathematical formalism the information coming from metabolic and functional images. The quadratic objective function, usually employed in commercial optimization algorithm, was generalized thus defining the present equation:

$$F = \sum_{\sigma=1}^{n_{\sigma}} \left\{ \frac{r_{\sigma}}{N_{\sigma}} \sum_{n=1}^{N_{\sigma}} r_n \cdot \left[D_c(n) - D_p(n) \right]^2 \right\}$$

where σ is an index to identify the structure, N_{σ} is the total number of voxels for the structure σ and $D_c(n)$ is the calculated dose at voxel n . If the voxel n belongs to the target, $D_p(n)$ represents the prescribed dose given by:

$$D_p(n) = D_p^0 + k \cdot M(n)$$

where D_p^0 is the conventional prescription dose when the functional image is not available, $M(n)$ is correlated with the metabolic information at voxel n , and k is an empirical coefficient.

By contrast, whenever the voxel n lies within normal tissue $D_p(n)$ then becomes a tolerance dose, $D_t(n)$, given by:

$$D_t(n) = D_t^0 - \alpha' \cdot K(n)$$

where D_t^0 is the conventional tolerance dose, $K(n)$ is correlated with the functional spatial information of the sensitive structure, and α' is an empirical coefficient. A linear relation between the metabolic information and the prescribed dose was assumed by Xing, but the formalism can be extended to any other relation. So this model makes it possible to define the appropriate dose prescription and tolerance dose for each voxel, replacing the simplistic assumption of a uniform dose within the target volume.

A similar approach was described by Alber [4.68], who proposed to transform the biological image (PET, fNMR, etc..) into a dose efficiency distribution, defining a linear calibration function with a prescribed maximum boost factor. A relative dose efficiency ($0 < < 1$) is introduced to represent the radiation effect on the tumour, at each voxel. So the optimization algorithm is forced to compensate for regionally variable radiosensitivity in order to achieve the minimum cost function value. The assumption is that the effective dose, given by the product , where represents the physical dose at point , should be homogeneous. Analogously, an effective dose-volume histogram may be plotted, to evaluate the plan in terms of biological information.

References

- 4.1 *A Practical Guide to Intensity-Modulated Radiation Therapy* 2003: Published in cooperation with members of the staff of Memorial Sloan-Kettering Cancer Center, Medical Physics, Publishing Madison, Wisconsin.
- 4.2 C Nutting, DP Dearnaley, S Webb "Intensity modulated radiation therapy: a clinical review." *Br J Radiol* 73:459-469; 2000.
- 4.3 IMRT CW Group "Intensity-modulated radiotherapy: current status and issues of interest." *Int J Radiat Oncol Biol Phys* 51 (4): 880-914; 2001.
- 4.4 *Intensity-Modulated Radiation Therapy: The state of art* 2003: AAPM, Medical Physics Monograph No. 29.
- 4.5 CM Ma, T Pawlicki, SB Jiang, JS Li, J Deng, E Mok, A Kapur, L Xing, L Ma and AL Boyer "Monte Carlo verification of IMRT dose distributions from a commercial treatment planning optimization system" *Phys Med Biol* 45:2483-2495; 2000.
- 4.6 R Jeraj, P Keall "Monte Carlo based inverse treatment planning" *Phys Med Biol* 44:1885-1896; 1999.
- 4.7 TD Solberg, JJ De Marco, FE Holly, JB Smathers and AA De Salles "Monte Carlo treatment planning for stereotactic radiosurgery" *Radiother Oncol* 49:73 - 84; 1998.
- 4.8 TR Mackie, JW Scrimger and JJ Battista "A convolution method of calculating dose for 15MV x-rays" *Med Phys* 12:188-196; 1985.
- 4.9 TR Mackie, AF Bielajew, DW Rogers and JJ Battista "Generation of photon energy deposition kernels using EGS Monte Carlo code" *Phys Med Biol* 33:1-20; 1988.
- 4.10 A Boyer, E Mok "A photon dose distribution model employing convolution calculations" *Med Phys* 12:169-177; 1985.
- 4.11 AL Boyer, YP Zhu, L Wang and P Francois "Fast Fourier transform convolution calculations of x-ray isodose distributions in homogeneous media" *Med Phys* 16:248-253; 1989.
- 4.12 Y Xiao, J Galvin, M Hossain, R Valicenti "An optimized forward planning technique for intensity modulated radiation therapy" *Med Phys* 27:2093-2099; 2000.
- 4.13 CX Yu, TR Mackie, JW Wong "Photon dose calculation incorporating explicit electron transport." *Med Phys* 22:1157-1165; 1995.
- 4.14 DWO Rogers, BA Faddegon, GX Ding, CM Ma, J We, TR Mackie "BEAM: A Monte Carlo code to simulate radiotherapy units" *Med Phys* 22:503-524; 1995.

- 4.15 F Verhaegen, J Seuntjens J. "Monte Carlo modelling of external radiotherapy photon beams" *Phys Med Biol* 48:R107–R164; 2003.
- 4.16 SY Jang, ON Vassiliev, HH Liu, R Mohan "Development and commissioning of a multileaf collimator model in MonteCarlo dose calculations for intensity-modulated radiation therapy" *Med Phys* 33(3):770-781; 2006.
- 4.17 IB Mihaylov, FA Lerma, Y Wu, JV Siebers "Analytic IMRT dose calculations utilizing Monte Carlo to predict MLC fluence modulation" *Med Phys* 33(4):828-839; 2006.
- 4.18 P Munro, JA Rawlingson, A Fenster "Therapy imaging: source size and radiotherapy beams" *Med Phys* 19:517-24;1988.
- 4.19 TC Zhu, BE Bjarmgaard, H Shackford "X/ray source and the output factor" *Med Phys* 22:793-8; 1995.
- 4.20 A Brahme "Geometric parameters of clinical electron beams" *Acta Radiologica* S364: 11-19; 1983.
- 4.21 P Bjork, T Knoos, P Nilsson "Influence of initial electron beam characteristics on Monte Carlo calculated absorbed dose distributions for linear accelerator of electron beams" *Phys Med Biol* 47: 4019; 2002.
- 4.22 M K Fix, P Manser, E J Born, R Mini, P Ruegsegger "Monte Carlo simulation of a dynamic MLC based on a multiple source model" *Phys Med Biol* 46:3241–3257; 2001.
- 4.23 P Francescon, S Cora, P Chiovati P "Verification of an IMRT treatment planning system with the BEAM EGS4-based Monte Carlo code" *Med Phys* 30(2):144-57; 2003.
- 4.24 S Chauvie, M Dominoni, P Marini, MG Pia, G Scielzo "Monte Carlo dose calculation algorithm on a distributed system" *Nucl Phys* 125S: 159-163; 2003.
- 4.25 S Webb. *The physics of conformal radiotherapy*. 1997: Institute of Physics (IOP) Bristol Publishing.
- 4.26 T Bortfeld "Optimized planning using physical objectives and constraints radiation therapy: The inverse, the converse and the perverse." *Sem Rad Oncol* 9:20-34; 1999.
- 4.27 M Mattia, P Del Giudice and B Caccia "IMRT optimization: variability of solutions and its radiobiological impact." *Med Phys* 31:1052–1060; 2004.
- 4.28 A Brahme "Treatment optimization using physical and radiobiological objective functions." In *Radiation Therapy Physics*, A. R. Smith (ed.), Springer-Verlag Berlin: 209–246; 1995.
- 4.29 S Webb "Optimization of conformal radiotherapy dose distributions by simulated annealing." *Phys Med Biol* 34(10):1349-1370; 1989.
- 4.30 Q Wu, R Mohan "Algorithms and functionality of an intensity modulated radiotherapy optimization system" *Med Phys* 27(4); 2000.
- 4.31 SV Spirou, and CS Chui "A gradient inverse planning algorithm with dose-volume constraints" *Med Phys* 25(3):321-333; 1998.
- 4.32 M Iori "Methods for physical and radiobiological optimization in radiotherapy with intensity modulation" *Phys Med* 17(2):55-73; 2001.
- 4.33 JO Desay "Multiple local minima in radiotherapy optimization problems with dose-volume constraints" *Med Phys* 24 (7): 1157–1161; 1997.
- 4.34 S Marzi, M Mattia, P Del Giudice, B Caccia and M Benassi "Optimization of intensity modulated radiation therapy: assessing the complexity of the problem." *Ann Ist Super Sanità* 37 (2): 225–230; 2001. On-line at <http://www.iss.it>.
- 4.35 CG Rowbottom, S Webb "Configuration space analysis of common cost functions in radiotherapy beam-weight optimization algorithms" *Phys Med Biol* 47(1):65–77; 2002.

- 4.36 Q Wu, and R Mohan "Multiple local minima in IMRT optimization based on dose-volume criteria." *Med Phys* 29 (7): 1514–1527; 2002.
- 4.37 SA Solla, GB Sorkin and SR White "Configuration space analysis for optimization problems." In *Disordered Systems and Biological Organization*. E. Bienenstock et al. (eds.) Berlin: Springer Verlag. 20 (F) 283–293; 1986.
- 4.38 SM Morrill, KS Lam, RG Lane, M Langer and II Rosen "Very fast simulated reannealing in radiation therapy treatment plan optimization." *Int J Radiat Oncol Biol Phys* 31(1) : 179-188; 1995.
- 4.39 M Alber, G Meedt, F Nüsslin and R Reemtsen "On the degeneracy of the IMRT optimization problem." *Med Phys* 29(11): 2584–2589; 2002.
- 4.40 B Caccia, P Del Giudice, S Marzi, M Mattia "IMRT optimization for head-neck case: variability of solutions and radiobiological evaluation" *Radiother Oncol* 73 (Suppl. 1): S342 - S343; 2004.
- 4.41 J L Verhey "Issues in optimization for planning of intensity-modulated radiation therapy" *Semin Radiat Oncol* 12(3): 210–218, 2002.
- 4.42 *Commissioning and Quality Assurance of Computerized Planning Systems for Radiation Treatment of Cancer* 2004: IAEA TRS No. 430, Vienna, Austria.
- 4.43 L Happersett, GS Mageras, MJ Zelefsky, CM Burman, SA Leibel "A study of the effects of internal organ motion on dose escalation in conformal prostate treatments" *Radiother Oncol* 66:263-270; 2003.
- 4.44 GS Mageras, Z Fuks, SA Leibel, CC Ling, MJ Zelefsky, HM Kooy, M van Herk and GJ Kutcher "Computerized design of target margins for treatment uncertainties in conformal radiotherapy" *Int J Radiat Oncol Biol Phys* 43:437-445; 1999.
- 4.45 V Moiseenko, J Battista, J Van Dick "Normal tissue complication probabilities: dependence on choice of biological model and dose-volume histogram reduction scheme" *Int J Radiat Oncol Biol Phys* 46:983-993; 2000.
- 4.46 B Emami, J Lyman, A Brown, L Coia, M Goitein, JE Munzenrider, B Shank, LJ Solin, M Wesson "Tolerance of normal tissue to therapeutic irradiation" *Int J Radiat Oncol Biol Phys* 21:109-122; 1991.
- 4.47 Q Wu, R Mohan, A Nimierko, R Schmit-Ullrich "Optimization of intensity-modulated radiotherapy plans based on the equivalent uniform dose" *Int J Radiat Oncol Biol Phys* 52:224-235; 2002.
- 4.48 C Fiorino, V Vavassori, G Sanguineti, C Bianchi, GM Cattaneo, A Piazzolla, C Cozzarini "Rectum contouring variability in patients treated for prostate cancer: impact on rectum dose-volume histograms and normal tissue complication probability" *Radiother Oncol* 63:249-255; 2002.
- 4.49 R Mohan, Q Wu, M Manning, R Schmit-Ullrich "Radiobiological considerations in the design of fractionation strategies for intensity-modulated radiation therapy of head and neck cancers" *Int J Radiat Oncol Biol Phys* 46:619-630; 2000.
- 4.50 R Ruggieri "Hypofractionation in non-small cell lung cancer (NSCLC): suggestions from modelling both acute and chronic hypoxia" *Phys Med Biol* 49:4811-4823; 2004.
- 4.51 C Clifton Ling, J Humm, S Larson, H Amols, Z Fuks, S Leibel, JA Koutcher "Towards multidimensional radiotherapy (MD-CRT): biological imaging and biological conformality" *Int J Radiat Oncol Biol Phys* 47:551-560; 2000.
- 4.52 JD Chapman, JD Bradley, JF Eary, R Haubner, SM Larson, JM Michalski, PG Okunieff, HW Strauss, YC Ung, MJ Welch "Molecular (functional) imaging for radiotherapy applica-

- tions: an RTOG symposium" *Int J Radiat Oncol Biol Phys* 55:294-301; 2003.
- 4.53 JS Rasey, W Koh, ML Evans, LM Peterson, TK Lewellen, MM Graham, KA Krohn "Quantifying regional hypoxia in human tumours with positron emission tomography of [¹⁸F] fluoromisonidazole: a pretherapy study of 37 patients" *Int J Radiat Oncol Biol Phys* 36:417-428; 1996.
- 4.54 KS Clifford Chao, WR Bosch, S Mutic, JS Lewis, F Dehdashti, MA Mintun, JF Dempsey, CA Perez, JA Purdy, MJ Welch "A novel approach to overcome tumour resistance: Cu-ATSM guided intensity-modulated radiation therapy" *Int J Radiat Oncol Biol Phys* 49:1171-1182; 2001.
- 4.55 J Kurhanewicz, DB Vigneron, H Hricak, P Carroll, P Narayan, S Nelson "Three-dimensional H-1 MR spectroscopic imaging of the in situ human prostate with high (0.24-0.7 cm³) spatial resolution" *Radiology* 198:795-805; 1996.
- 4.56 WA Tomé, JF Fowler "Selective boosting of tumour subvolumes" *Int J Radiat Oncol Biol Phys* 48:593-599; 2000.
- 4.57 JO Deasy "Partial tumour boost: even more attractive than theory predicts?" *Int J Radiat Oncol Biol Phys* 51:279-282; 2001.
- 4.58 D Levin-Plotnik, RJ Hamilton "Optimization of tumour control probability for heterogeneous tumours in fractionated radiotherapy treatment protocols" *Phys Med Biol* 49:407-424; 2004.
- 4.59 RA Popple, R Ove, S Shen "Tumour control probability for selective boosting of hypoxic subvolumes, including the effect of reoxygenation" *Int J Radiat Oncol Biol Phys* 54:921-927; 2002.
- 4.60 PL Olive, JP Banàth, C Aquino-Parsons "Measuring hypoxia in solid tumors" *Acta Oncol* 40:917-923; 2001.
- 4.61 HLK Janssen, KMG Haustermans, D Sprong, G Blommestijn, I Hofland, FJ Hoebbers, E Blijweert, JA Raleigh, GL Semenza, MA Varia, AJ Balm, MF van Velthuysen, P Delaere, R Scot, AC Begg "HIF-1A, Pimonidazole, and Iododeoxyuridine to estimate hypoxia and perfusion in human head-and-neck tumors" *Int J Radiat Oncol Biol Phys* 54:1537-1549; 2002.
- 4.62 GO De Meerleer, LAML Vakaet, WRT De Gersem, C De Wagter, B De Naeyer, W De Neve "Radiotherapy of prostate cancer with or without intensity modulated beams: A planning comparison" *Int J Radiat Oncol Biol Phys* 47:639-648; 2000.
- 4.63 WRT De Gersem, S Derycke, CO Colle, C De Wagter, WJ De Neve "Inhomogeneous target dose distributions: A dimension more for optimization?" *Int J Radiat Oncol Biol Phys* 44:461-468; 1999.
- 4.64 A Niemierko "Reporting and analyzing dose distributions: a concept of equivalent uniform dose" *Med Phys* 24:103-110; 1997.
- 4.65 MA Ebert "Viability of the EUD and TCP concepts as reliable dose indicators" *Phys Med Biol* 45:441-457; 2000.
- 4.66 H Amols, C Ling "EUD but not QED" *Int J Radiat Oncol Biol Phys* 52:1-2; 2002.
- 4.67 L Xing, C Cotrutz, S Hunjan, AL Boyer, E Adalsteinsson, D Spielman "Inverse planning for functional image-guided intensity-modulated radiation therapy" *Phys Med Biol* 47:3567-3578; 2002.
- 4.68 M Alber, F Paulsen, SM Eschmann, HJ Machulla "On biologically conformal boost dose optimization" *Phys Med Biol* 48: N31-N35; 2003.

Acknowledgements

The coordinator and all the members of the IMRT-AIFM group express their thanks and appreciations to Mrs. Verlie Jones, radiographer at the Istituto Europeo di Oncologia di Milano, who has kindly accepted to review the English language of this report.